Power series expansion of the Jost function on the complex angular momentum plane

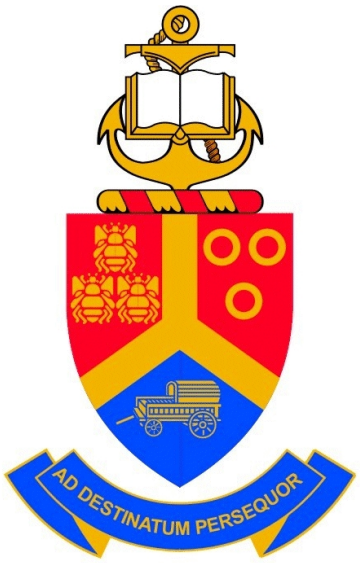

by

John Tshegofatso Tshipi

Submitted in partial fulfilment of the requirements for the degree

Magister Scientiae

In the Faculty of Natural & Agricultural Sciences
University of Pretoria
Pretoria

Supervisor: Prof. Sergei Rakitianski

2016

UNIVERSITY OF PRETORIA

DECLARATION OF ORIGINALITY

This document must be signed and submitted with every essay, report, project, assignment, dissertation and/or thesis.

Full names of student: John Tshegofatso Tshipi

Student number: 27460054

Declaration

1. I understand what plagiarism is and am aware of the University's policy in this regard.
2. I declare that this thesis is my own original work. Where other people's work has been used (either from a printed source, Internet or any other source), this has been properly acknowledged and referenced in accordance with departmental requirements.
3. I have not used work previously produced by another student or any other person to hand in as my own.
4. I have not allowed, and will not allow, anyone to copy my work with the intention of passing it off as his or her own.

SIGNATURE STUDENT:.....

SIGNATURE SUPERVISOR:.....

Abstract

The aim of this research is to develop a method for expanding the Jost functions as a Taylor-type power series on the complex angular momentum plane. From this method in conjunction with the Watson transformation, we were able to express the scattering amplitude as a sum of the background and pole terms, furthermore, this method propose a way of evaluating, numerically, the pole term. To demonstrate how this method may be applied, we considered the Born approximation. We found out that the developed method improved the Born approximation at large scattering angles. Therefore, this method is useful when the differential cross section of the background term fails to converge to that of the exact differential cross section at large scattering angles.

Acknowledgments

First and foremost I thank God for creating me as well as allowing me to prosper on this planet.

Secondly, I like to extend my deepest gratitude to Prof. Sergei Rakitianski for giving me the opportunity to study under him. Furthermore, I thank him also for his patience, help and guidance as well introducing me to the fascinating world of Scattering theory and FORTRAN.

Finally, I thank the National Research Foundation for their financial support and my family for being my pillar of moral support.

Contents

List of Figures

List of Tables

Chapter 1

Introduction

"Much of our understanding about the structure of matter is extracted from the scattering of particles. Had it not been for scattering, the structure of the microphysical world would have remained inaccessible to humans. It is through scattering experiments that important building blocks of matter, such as the atomic nucleus, the nucleons, and the various quarks, have been discovered." $\sim$ Nouredine Zettili [1].

As a motivation to this quote, Basdevant and Dalibard [2] gave the following applications of scattering; Rutherford's experiment, which was based on the scattering of α particles by gold atoms, proved the existence of a nucleus with a positive charge and a size of 10^5 times smaller than the atomic radius. Modern laser spectroscopy, which provides information on the structure of atoms and molecules, may be considered as a photon scattering process. The scattering of conduction electrons by impurities in the crystal, provides us with the information to understand quantitatively the electric conductivity of a metal. And they further wrote, Particles that are incident at very large energies, by modern accelerators, allow us to examine matter thoroughly at short distances ($\leq 10^{-18}$m), therefore, particle physics is based on the anal-

ysis of scattering processes.

The cross section measures how much of the incident particles would be scattered by the potential into a solid angle, is an observable quantity, meaning it can be obtained experimentally. In classical scattering, we have an incident particle with energy E and impact parameter b, that is deflected by the potential and emerges at an angle θ, that is known as a scattering angle.

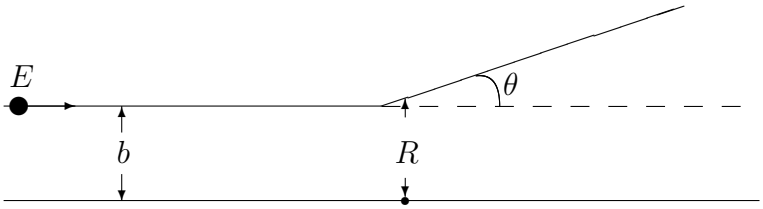

Figure 1.1: Classical view of scattering-Particle with energy E and impact b incident towards a potential with range R and scattering angle θ

The scattering angle θ is the angle between the incoming and outgoing trajectory. This scattering angle depends on the incident energy, E, as well as the impact parameter,b. For example, for fixed energies and $b < R(b > R)$, where R is the range of the potential, the scattering angle will be large(small). For high energies and fixed b, the particle will spent less time around the potential as a result θ would be small. Therefore for a spherical symmetric potentials, the differential cross section is expressed as

$$\frac{d\sigma}{d\Omega} = \frac{b}{\sin\theta}\left|\frac{db}{d\theta}\right|. \tag{1.1}$$

Thus we can calculate the differential cross sectional (1.1) if, for a given energy, we know the impact parameter b. According to [3], Eq. (1.1) holds only if the de Brogile wavelength of the incident particle is smaller than the dimensions of the scattering region. As the de Brogile wavelength increases, quantum uncertainty starts to restrict us from knowing simultaneously both the momentum and position (which can be related to impact parameter) of the beam. As a consequence, we now move from the classical regime to a quantum one. For the latter regime, calculations are made by considering the wave characteristics of the particle.

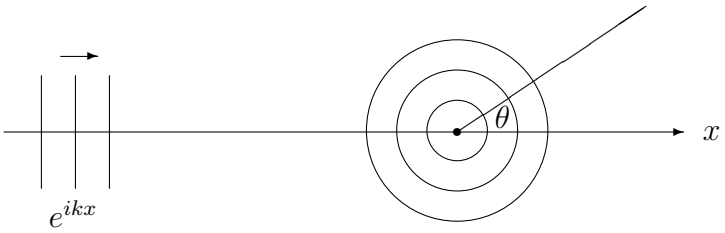

Figure 1.2: Quantum scattering- A plane wave with momentum k that is scattered spherical outwards and an angle θ

In quantum scattering, instead of beam of particles, we have a plane wave with energy E which moves towards the potential, after the wave-potential interaction the plane wave is transformed into a spherical outgoing wave [4]. For quantum scattering, the differential cross-sectional area for symmetric potentials is expressed as

$$\frac{d\sigma}{d\Omega} = |f(\theta)|^2 . \tag{1.2}$$

We can calculate the cross section (1.2) if, for a given energy and scattering angle θ, we know the scattering amplitude $f(\theta)$ - which is calculated by

solving the Schödinger equation [4]. The scattering amplitude represents the probability of scattering in the direction of the angle θ.

There are numerous approaches dedicated for the calculation of the scattering amplitude, as it can be seen in [5], amongst others, there is the Born approximation [1], which is useful when the incident beam has high energies or experiences weak scattering potentials. High energies implies that the average interaction between the incident particle and the potential will be small, as a result the scattering angle will also be small and thus the scattered wave may be approximated to be the incident plane wave.

According to [5], the method of partial wave analysis expresses the scattering amplitude as a series where the summation variable is the orbital angular-momentum quantum number(ℓ),

$$f(\theta) = \sum_{\ell=0}^{\infty} (2\ell + 1) f_\ell(E) P_\ell(\cos\theta). \tag{1.3}$$

This method is valid for low energies and finite range potentials - if the range of the potential is R and k is the momentum (or wave number) of the particle, then the partial waves that would contribute to scattering will be such that

$$\ell \leq kR.$$

Last but not least, is the semi-classical method [5] which is valid when the de Brogile wavelength of the incident particle is short compared to the range of the potential. For a potential of range R and incident energy k, the semi-classical condition is

$$kR \gg 1.$$

The scattering amplitude is expressed in terms of a series of partial waves

(PW) with the variable being a non-negative integer, this series is slowly convergent. The Complex Angular-Momentum approach (CAM), as the name suggests, allows the angular momentum to assume complex values and when it is coupled with the Watson transformation - which converts the infinite partial wave series into a contour integral - PW series and thus the scattering amplitude is represented as a sum of pole terms and a background integral, which converges faster than the series.

T. Tamura and H.H Wolter [7], investigated the analytic continuation of the S-matrix in the complex ℓ plane for the Woods-Saxon optical potential. They studied exact behavior of the pole and background terms. They observed that for elastic scattering, models that uses background-single-pole reproduce the scattering amplitute accurately for sufficiently high energies and the system treated was strongly absorptive.

The scattering amplitude is mostly, if not always, expressed as a partial wave series for elastic collisions[6]-[8]. Furthermore, it is also expressed as a sum of the background term and the pole sum. Connor [6], calculates the Regge poles and residues using the semi-classical (WKB) approximation technique for diffraction scattering in atom-atom scattering and observed that for diffraction scattering in atom-atom collisions, the differential cross-section of the partial wave with the summation of several hundreds may be fully expressed as the sum of the background integral and a single pole, where the error between the CAM approach and the experimental data was very small. Moreover, observed that the CAM technique explains diffraction scattering well if the absolute value of the residue have magnitudes of order unity i.e less than 10.

The main idea of this thesis is to develop a method for expanding the Jost

functions as a power series in the complex angular momentum plane. We demostrate the application of this method by considering the Born approximation. We further found out that this method improved the Born approximation at large scattering angles.

This thesis is organised as follows.

- Chapter 2 we do the following:
  - Section 2.1, starts by defining Jost functions and how they are calculated.
  - Section 2.2, we define Regge poles as well as Regge trajectories and determine where these poles are located in the complex angular momentum plane.
  - Section 2.3, we prove that the Jost functions are analytic with respect to the angular momentum parameter. Afterwards obtain the power series expansion of the Jost functions for short range potentials.
- Chapter 3, we define scattering amplitude and relate it to the differential cross section.
- Chapter 4, we demostrate with an example of how the developed method may be used in applications.
- Chapter 5, we compare the results of the exact differential cross section to that of the partial wave method as well as that of the complex angular momentum method.
- Chapter 6 is the conclusion.

Chapter 2

Theory

2.1 Jost function

The bound, scattering and resonance states are three physical problems that are associated with the Schröndger equation. The difference between these states is the boundary condition imposed on the wave function at large distances. The description of these states can be unified by using the Jost function approach. Jost functions, which are purely mathematical entities, have an extraordinary property, their zeros in the complex angular momentum plane are exactly at those values of the momentum at which the system has bound, scattering and resonance states. In essence, these functions offer an exquisite way of solving physical problems by locating those zeros. In this section, we will derive differential equations for calculating the Jost functions and provide a definition of a power series.

2.1.1 Calculations of the Jost functions

In order for us to find a way of calculating the Jost function, we start by solving the the radial Schrödinger equation

$$\left[\frac{d^2}{dr^2} + k^2 - \frac{l(l+1)}{r^2}\right] u_l(E,r) = V(r)u_l(E,r), \tag{2.1}$$

by the variation parameter method (Appendix A), where $u_l(E,r)$ represents the radial wave function,

$$u_l(E,r) = h_l^{(-)}(kr)F_l^{(in)}(E,r) + h_l^{(+)}(kr)F_l^{(out)}(E,r). \tag{2.2}$$

At large distances the potential energy vanishes and the wave function behaves like a linear combination of the Riccati-Hankel functions satisfying the equation

$$\left[\frac{d^2}{dr^2} + k^2 - \frac{l(l+1)}{r^2}\right] h_l^{(\pm)}(kr) = 0. \tag{2.3}$$

In Eq. (2.2), the wave function $u_l(E,r)$ is expressed in terms of two unknown functions $F_l^{(in)}(E,r)$ and $F_l^{(out)}(E,r)$ which are related to each other. We can impose an arbitrary condition that describes the relationship between $F_l^{(in)}(E,r)$ and $F_l^{(out)}(E,r)$. Let that relationship be

$$h_l^{(-)}(kr)\partial_r F_l^{(in)}(E,r) + h_l^{(+)}(kr)\partial_r F_l^{(out)}(E,r) = 0. \tag{2.4}$$

The condition (2.4) is known as the Lagrange condition. When (2.2) is substituted into (2.1), the first term becomes

$$\begin{aligned}\frac{d^2}{dr^2}u_l(E,r) = &\frac{d}{dr}\left[\partial_r h_l^{(-)}(kr)F_l^{(in)}(E,r) + h_l^{(-)}(kr)\partial_r F_l^{(in)}(E,r)\right] \\ &+ \frac{d}{dr}\left[\partial_r h_l^{(+)}(kr)F_l^{(out)}(E,r) + h_l^{(+)}(kr)\partial_r F_l^{(out)}(E,r)\right],\end{aligned} \tag{2.5}$$

then applying (2.4) to Eq. (2.5),

$$\frac{d^2}{dr^2}u_l(E,r) = \frac{d}{dr}\left[\partial_r h_l^{(-)}(kr)F_l^{(in)}(E,r) + h_l^{(+)}(kr)\partial_r F_l^{(out)}(E,r)\right]. \quad (2.6)$$

Rewriting (2.1) in terms of (2.6):

$$\left[\frac{d^2}{dr^2} + k^2 - \frac{l(l+1)}{r^2}\right]\left[h_l^{(-)}(kr)F_l^{(in)}(E,r) + h_l^{(+)}(kr)F_l^{(out)}(E,r)\right]$$
$$+ \partial_r h_l^{(-)}(kr)\partial_r F_l^{(in)}(E,r) + h_l^{(+)}(kr)\partial_r F_l^{(out)}(E,r) = V(r)u_l(E,r), \quad (2.7)$$

substituting (2.3) into (2.7):

$$\partial_r h_l^{(-)}(kr)\partial_r F_l^{(in)}(E,r) + \partial_r h_l^{(+)}(kr)\partial_r F_l^{(out)}(E,r) = V(r)u_l(E,r), \quad (2.8)$$

writing (2.4) as

$$h_l^{(-)}(kr)\partial_r F_l^{(in)}(E,r) = -\partial_r h_l^{(+)}(kr)\partial_r F_l^{(out)}(E,r). \quad (2.9)$$

Then (2.8) becomes

$$\partial_r h_l^{(-)}(kr)\partial_r F_l^{(in)}(E,r) - \frac{h_l^{(-)}(kr)}{h_l^{(+)}(kr)}\partial_r h_l^{(+)}(kr)\partial_r F_l^{(in)}(E,r) = V(r)u_l(E,r). \quad (2.10)$$

Thus

$$-\frac{1}{h_l^{(+)}(kr)}\left[h_l^{(-)}(kr)\partial_r h_l^{(-)}(kr) - h_l^{(+)}(kr)\partial_r h_l^{(+)}(kr)\right]\partial_r F_l^{(in)}(E,r)$$
$$= V(r)u_l(E,r). \quad (2.11)$$

The Wronskian of the Riccati-Hankel function is known as

$$h_l^{(-)}(kr)\partial_r h_l^{(+)}(kr) - h_l^{(+)}(kr)\partial_r h_l^{(-)}(kr) = 2ik. \tag{2.12}$$

Then substituting (2.12) into (2.14), we obtain

$$-\frac{1}{h_l^{(+)}(kr)}\,(2ik)\,\partial_r F_l^{(in)}(E,r) = V(r)u_l(E,r), \tag{2.13}$$

similarly, for $\partial_r F_l^{(out)}(E,r)$ we obtain

$$\frac{1}{h_l^{(-)}(kr)}\,(2ik)\,\partial_r F_l^{(out)}(E,r) = V(r)u_l(E,r), \tag{2.14}$$

where $u_l(E,r)$ was defined in (2.2). Therefore, the first-order coupled differential equations for the new unknown functions are as follows :

$$\partial_r F_l^{(in)}(E,r) = -\frac{h_l^{(+)}(kr)}{2ik}V(r)\left[h_l^{(-)}(kr)F_l^{(in)}(E,r) + h_l^{(+)}(kr)F_l^{(out)}(E,r)\right] \tag{2.15}$$

$$\partial_r F_l^{(out)}(E,r) = \frac{h_l^{(-)}(kr)}{2ik}V(r)\left[h_l^{(-)}(kr)F_l^{(in)}(E,r) + h_l^{(+)}(kr)F_l^{(out)}(E,r)\right]. \tag{2.16}$$

Equations (2.15) and (2.16) are equivalent to the radial Schrödinger equation (2.1). When the potential, V, vanishes at $r > R$, the right hand side (RHS) of (2.15) and (2.16) becomes zero. As a result the unknown functions $F_l^{(in)}(E,r)$ and $F_l^{(out)}(E,r)$ become constants. The form (2.2) ensures that the solutions have correct asymptotic behaviour outside the interaction region. $h_l^{(-)}(kr)$ and $h_l^{(+)}(kr)$ are singular at $r = 0$, but those singularities cancel each other, if they are superimposed

$$h_l^{(-)}(z) + h_l^{(-)}(z) = 2j_l(z). \tag{2.17}$$

This is achieved when both $F_l^{(in)}(E,r)$ and $F_l^{(out)}(E,r)$ have the same value at $r=0$, i.e

$$F_l^{(in)}(E,0) = F_l^{(out)}(E,0). \tag{2.18}$$

Since we are not concerned with their normalization, then

$$F_l^{(in/out)}(E,0) = 1. \tag{2.19}$$

Comparing (2.2) with the corresponding asymptotic behaviour

$$u_l(E,r) \underset{r\to\infty}{\longrightarrow} h_l^{(-)}(kr) f_l^{(in)}(E) + h_l^{(+)}(kr) f_l^{(out)}(E), \tag{2.20}$$

it follows that

$$f_l^{(in)}(E) = \lim_{r\to\infty} F_l^{(in)}(E,r), \tag{2.21}$$

and

$$f_l^{(out)}(E) = \lim_{r\to\infty} F_l^{(out)}(E,r). \tag{2.22}$$

The superscripts *in* and *out* mean incoming and outgoing functions, respectively. Eqs. (2.21)-(2.22) are the Jost functions and in order to calculate them, we have to determine first the unknown functions $F^{(in/out)}$ from (2.15)-(2.16) at large values of distance r.

2.1.2 Power series expansion

If a function $f(z)$ is analytic(differentiable) at the point p, which is contained in the domain of a complex plane D i.e $p \in D$, then the Taylor-type power series about the point p is given by [9]

$$f(z) = \sum_{n=0}^{n} a_n (z-p)^n, \tag{2.23}$$

where

$$a_n = \frac{f^{(n)}(p)}{n!}, \quad \text{for } n \geq 0$$

are known as the expansion coefficients of the power series.

Therefore, to obtain a power series of the Jost functions for fixed energies and arbitrary complex angular momenta, we have to choose an arbitrary point in some domain D, in the complex angular momentum(CAM) plane and do an expansion about that point.

2.2 Location of the Regge Poles

In this thesis we will be working only with scattering states. The energy of this state is real and positive. For us to obtain a power series expansion of the Jost functions in the complex angular momentum plane, we have to determine in which quadrant the scattering states are located. Thus, this will be the objective for this section.

For a fixed value of the energy, the poles of the S-matrix, which are such that $f_\ell^{(in)}(E) = 0$, in the complex angular momentum plane are called the Regge poles [5]. A Regge pole is a complex number

$$\ell = \ell_r + i\ell_I, \tag{2.24}$$

where ℓ_r denotes the real part of ℓ and ℓ_I the imaginary part. A curve that is traced out when the Regge pole moves, as a result of increasing energy, in the complex ℓ-plane is called the Regge trajectory. This trajectories play an important role, since they determine where a resonance and bound state occur in the CAM plane, i.e the former occur when $E > 0$ and ℓ_r is equal to a non-negative integer and ℓ_I must be very small, whereas the latter also

occur when ℓ_r is equal to a non-negative integer but $E < 0$ [5].

Regge trajectories may consist of both bound and resonance spectral points. Thus, by obtaining this trajectory it would be possible to determine at which energies and partial waves a bound or resonance state must exist [14]. The radial wave function for a stationary scattering state at large distances is given by

$$u(E,r) \quad \underset{r\to\infty}{\longrightarrow} \quad h_\ell^{(-)}(kr) f_\ell^{(in)}(E) + h_\ell^{(+)}(kr) f_\ell^{(out)}(E). \tag{2.25}$$

For Regge poles $f_\ell^{(in)}(E) = 0$ must hold, hence (2.25) becomes

$$\begin{aligned} u_\ell(E,r) \quad &\underset{r\to\infty}{\longrightarrow} \quad h_\ell^{(+)}(kr) f_\ell^{(out)}(E) \\ &\underset{r\to\infty}{\longrightarrow} \quad \left[-ie^{i(kr-\ell\frac{\pi}{2})}\right] f_\ell^{(out)}(E) \\ &\underset{r\to\infty}{\longrightarrow} \quad \exp\left[i(kr - \frac{\pi}{2}(\mathrm{Re}(\ell)+1)) + \frac{\pi}{2}\mathrm{Im}(\ell)\right] f_\ell^{(out)}(E), \end{aligned} \tag{2.26}$$

in eq. (2.26) we used the fact that

$$-i = \exp(-i\pi/2).$$

The boundary condition of the wave function is given as

$$u_\ell(E,0) = 0. \tag{2.27}$$

For complex values of ℓ, the Schrödinger equation becomes

$$\left[\frac{d^2}{dr^2} + k^2 - \frac{\ell\,(\ell+1)}{r^2} - V(r)\right] u_\ell(E,r) = 0, \tag{2.28}$$

where

$$\begin{aligned}\frac{\ell(\ell+1)}{r^2} &= \frac{\mathrm{Re}(\ell(\ell+1)) + i\,\mathrm{Im}(\ell(\ell+1))}{r^2} \\ &= \frac{(\mathrm{Re}\ell+1)\mathrm{Re}\ell - (\mathrm{Im}\ell)^2}{r^2} + i\,\frac{(2\mathrm{Re}\ell+1)\mathrm{Im}\ell}{r^2}.\end{aligned} \tag{2.29}$$

If k is real, then its complex conjugate is real and this implies that k^2 will be real too. Therefore

$$\left[\frac{d^2}{dr^2} + k^2 - \frac{1}{r^2}\mathrm{Re}[\ell(\ell+1)] + i\,\frac{1}{r^2}\mathrm{Im}[\ell(\ell+1)] - V(r)\right] u_\ell(E,r) = 0, \tag{2.30}$$

$$\left[\frac{d^2}{dr^2} + k^2 - \frac{1}{r^2}\mathrm{Re}[\ell(\ell+1)] - i\,\frac{1}{r^2}\mathrm{Im}[\ell(\ell+1)] - V(r)\right] u^*_{\ell*}(E,r) = 0. \tag{2.31}$$

Eq. (2.31) was obtained by taking a the complex conjugate of Eq. (2.30). $u^*_{\ell*}(E,r)$ is the complex conjugate of $u_\ell(E,r)$.
Multiplying (2.30) and (2.31) by $u^*_{\ell*}(E,r)$ and $u_\ell(E,r)$, respectively, and then substract (2.31) from (2.30) results,

$$\begin{aligned}2\,i\,\mathrm{Im}[\ell(\ell+1)]\frac{|u_\ell(E,r)|^2}{r^2} &= u^*_{\ell*}u''_\ell - (u^*_{\ell*})''u_\ell \\ &= \frac{\mathrm{d}}{\mathrm{d}r}\left[u^*_{\ell*}u'_\ell - (u^*_{\ell*})'u_\ell\right],\end{aligned} \tag{2.32}$$

where u' and u'' are the first and second derivative with respect to r. Since for scattering states the momentum k is real, then it follows that at large distances Eq. (2.26) is pure oscillatory and thus it is bounded, i.e $|u_\ell(E,r)| < M$. As a result we have

$$0 < \int_0^\infty \frac{|u_\ell(E,r)|^2}{r^2}\,dr < \infty, \tag{2.33}$$

$$u_\ell(E,r) \quad \underset{r\to\infty}{\longrightarrow} \quad \exp\left[i(kr-\frac{\pi}{2}(\mathrm{Re}(\ell)+1))+\frac{\pi}{2}\mathrm{Im}(\ell)\right] f_\ell^{(out)}(E),$$

$$u_{\ell^*}^*(E,r) \quad \underset{r\to\infty}{\longrightarrow} \quad \exp\left[-i(kr-\frac{\pi}{2}(\mathrm{Re}(\ell)+1))+\frac{\pi}{2}\mathrm{Im}(\ell)\right] f_{\ell^*}^{(out)*}(E), \tag{2.34}$$

$$u_\ell'(E,r) \quad \underset{r\to\infty}{\longrightarrow} \quad ik\exp\left[i(kr-\frac{\pi}{2}(\mathrm{Re}(\ell)+1))+\frac{\pi}{2}\mathrm{Im}(\ell)\right] f_\ell^{(out)}(E), \tag{2.35}$$

$$(u_{\ell^*}^*(E,r))' \quad \underset{r\to\infty}{\longrightarrow} \quad -ik\exp\left[-i(kr-\frac{\pi}{2}(\mathrm{Re}(\ell)+1))+\frac{\pi}{2}\mathrm{Im}(\ell)\right] f_{\ell^*}^{(out)*}(E). \tag{2.36}$$

Integrating both sides of (2.32) and taking into account (2.27) as well as substituting (2.34) - (2.36) into the RHS of (2.32) gives

$$\mathrm{Im}\left[\ell(\ell+1)\right]\int_0^\infty \frac{|u_\ell(E,r)|^2}{r^2}\,dr = k|f_\ell^{(out)}(E)|^2 e^{\pi \mathrm{Im}\,\ell}. \tag{2.37}$$

All other factors in (2.37) are positive, therefore

$$\mathrm{Im}\left[\ell(\ell+1)\right] > 0.$$

For spectral points, $\mathrm{Re}\,\ell \geq 0$, we conclude that

$$\mathrm{Im}\,\ell > 0.$$

Therefore, the Regge poles for scattering are located in the first quadrant of the complex angular momentum plane.

2.3 Analyticity of the Jost function

In section 2.2, we have shown that the Regge poles for scattering are located in the first quadrant of the CAM plane. The next step towards expressing the Jost function as power series of ℓ is to show that the Jost functions are analytic inside some arbitrary circle.

To obtain the power series expansion of the Jost functions, we start by choosing an arbitrary point, ℓ_0, in the first quadrant of the complex angular momentum plane. Then we do a power series expansion about that point in the circle, γ, as shown in Fig. (2.1).

We now show that the solutions of the differential equations (2.15) and (2.16) are analytic with respect to the parameter ℓ. To prove analyticity, we use the Poincarè theorem.
This theorem say that, at every fixed r a solution $\varphi(\zeta, r)$ of the differential equation

$$\frac{d^2}{dr^2}\varphi(\zeta, r) + J(\zeta, r)\frac{d}{dr}\varphi(\zeta, r) + K(\zeta, r)\varphi(\zeta, r) = 0, \tag{2.38}$$

where $J(\zeta, r)$ and $K(\zeta, r)$ are analytical functions of the parameter ζ, is an entire function of this parameter if the boundary conditions $\varphi(\zeta, r_0)$ and $\partial_r\varphi(\zeta, r_0)$ at a regular point r_0 are independent of ζ.

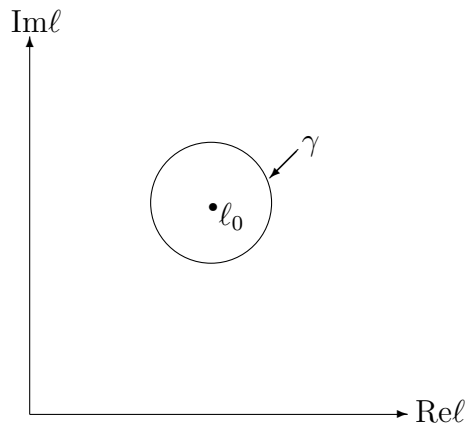

Figure 2.1: An arbitrary point ℓ_0 inside the circle γ in the complex angular momentum plane

From the boundary condition (2.19), we obtain

$$F_\ell^{(in/out)}(E,0) = 1, \tag{2.39}$$

where $r = 0$ is a regular point. Applying the Poincaré theorem on (2.39), we conclude that the functions $F_\ell^{(in/out)}(E,0)$ are analytic with respect to the parameter ℓ. Now, we have to show that the coefficients, $h_\ell^{(\pm)}(kr)$, are analytic with respect to the parameter ℓ as well.

The Riccati-Hankel functions $h_\ell^{(\pm)}(kr)$ are defined as

$$h_\ell^{(\pm)}(kr) = j_\ell(kr) \pm i n_\ell(kr), \tag{2.40}$$

where $j_\ell(kr)$ and $n_\ell(kr)$ are know as the Riccati-Bessel and Riccati-Neumann functions, respectively. These two Riccati functions are linearly independent, which means that

$$j_\ell(kr) \neq c n_\ell(kr),$$

for any constant c.

The Riccati-Bessel and Riccati-Neumann functions are solutions of the 'free' Schrödinger equation

$$\left[\frac{d^2}{dr^2} + k^2 - \frac{\ell\,(\ell+1)}{r^2}\right] u_\ell(E,r) = 0, \tag{2.41}$$

where $u_\ell(E,r) = h_\ell^{(\pm)}(kr) = j_\ell(kr) \pm i n_\ell(kr)$ and

$$j_\ell(kr) = \left(\frac{\pi(kr)}{2}\right)^{\frac{1}{2}} J_{\ell+\frac{1}{2}}(kr), \tag{2.42}$$

and

$$n_\ell(kr) = \left(\frac{\pi(kr)}{2}\right)^{\frac{1}{2}} Y_{\ell+\frac{1}{2}}(kr). \tag{2.43}$$

$J_{\ell+\frac{1}{2}}(kr)$ and $Y_{\ell+\frac{1}{2}}(kr)$ are respectively known as the Bessel and Neumann functions, which are defined as

$$J_v(z) = \frac{\left(\frac{z}{2}\right)^v}{\pi^{\frac{1}{2}}} \int_0^\pi \cos(z\cos(\theta)) \sin^{2v}(\theta)\, \mathrm{d}\theta, \tag{2.44}$$

$$Y_v(z) = \frac{J_v(z)\cos(\pi v) - J_{-v}(z)}{\sin(\pi v)}, \tag{2.45}$$

for non-integer values of v.

The boundary conditions for Eq. (2.41) are

$$j_\ell(kr) \quad \underset{r\to 0}{\longrightarrow} \quad \frac{(kr)^{\ell+1}}{\prod_{i=1}^{\ell}(2i+1)}, \tag{2.46}$$

and

$$n_\ell(kr) \quad \underset{r\to 0}{\longrightarrow} \quad (kr)^{-\ell}\prod_{i=1}^{\ell}(2i-1). \tag{2.47}$$

The problem with equations (2.46) and (2.47) is, both of them depend on ℓ and as a result the Poincarè theorem can not be employed. In order to circumvent this problem we re-normalize (2.46) and (2.47);

$$\tilde{j}_\ell(kr) = \frac{\prod_{i=1}^{\ell}(2i+1)}{(kr)^\ell} j_\ell(kr) \quad \underset{r\to 0}{\longrightarrow} \quad kr \tag{2.48}$$

$$\tilde{n}_\ell(kr) = \frac{(kr)^\ell}{\prod_{i=1}^{\ell}(2i-1)} n_\ell(kr) \quad \underset{r\to 0}{\longrightarrow} \quad 1 \tag{2.49}$$

Note: the function $\tilde{j}_\ell(kr)$ has the same analytic properties as $j_\ell(kr)$, except for the point $k=0$, and also $\tilde{n}_\ell(kr)$ has the same properties as $n_\ell(kr)$.

Then

$$\partial_r \tilde{j}_\ell(kr) \quad \underset{r\to 0}{\longrightarrow} \quad k, \tag{2.50}$$

$$\partial_r \tilde{n}_\ell(kr) \quad \underset{r\to 0}{\longrightarrow} \quad 0. \tag{2.51}$$

The re-normalized equations (2.48)-(2.51) are independent of the parameter ℓ.

We rewrite (2.48) and (2.49) as;

$$j_\ell(kr) = \frac{(kr)^\ell}{c_1}\tilde{j}_\ell(kr), \tag{2.52}$$

and

$$n_\ell(kr) = c_2(kr)^{-\ell}\tilde{n}_\ell(kr), \tag{2.53}$$

where

$$c_1 = \prod_{i=1}^{\ell}(2i+1),$$

and

$$c_2 = \prod_{i=1}^{\ell}(2i-1).$$

To show that $j_\ell(kr)$ and $n_\ell(kr)$ are analytic, we only need to show that the product on the RHS of (2.52) and (2.53) are analytic functions of ℓ.

$(kr)^\ell$ and $(kr)^{-\ell}$ are analytic, since they are differentiable with respect to ℓ at every point, except for $r = 0$ in the case of (2.53).

Then from (2.52):

$$\partial_r j_\ell(kr) = \frac{1}{c_1}\left(\frac{\ell(kr)^\ell}{r}\tilde{j}_\ell(kr) + (kr)^\ell\partial_r\tilde{j}_\ell(kr)\right).$$

$$\partial_r^2 j_\ell(kr) = \frac{1}{c_1}\left(\frac{(\ell^2-\ell)\,(kr)^\ell}{r^2}\tilde{j}_\ell(kr) + 2\ell\frac{(kr)^\ell}{r}\partial_r\tilde{j}_\ell(kr) + (kr)^\ell\partial_r^2\tilde{j}_\ell(kr)\right). \tag{2.54}$$

Substituting (2.54) into (2.41)

$$\begin{aligned}\frac{(kr)^\ell}{c_1}\left(-\frac{\ell(1-\ell)}{r^2}\tilde{j}_\ell(kr) + \frac{2\ell}{r}\partial_r\tilde{j}_\ell(kr) + \partial_r^2\tilde{j}_\ell(kr)\right)\\ +\frac{(kr)^\ell}{c_1}\left(k^2\tilde{j}_\ell(kr) - \frac{\ell\,(\ell+1)}{r^2}\tilde{j}_\ell(kr)\right) = 0,\end{aligned} \tag{2.55}$$

multiply (2.55) by

$$\frac{c_1}{(kr)^\ell}$$

$$\begin{aligned}\left[\partial_r^2 + k^2 - \frac{\ell\,(\ell+1)}{r^2}\right]\tilde{j}_\ell(kr) + \frac{2\ell}{r}\partial_r\tilde{j}_\ell(kr) - \frac{\ell(1-\ell)}{r^2}\tilde{j}_\ell(kr) = 0 \\ \partial_r^2\tilde{j}_\ell(kr) + \left[\frac{2\ell}{kr}\partial_r + 1 - \frac{2\ell}{(kr)^2}\right]\tilde{j}_\ell(kr) = 0,\end{aligned} \tag{2.56}$$

similarly from (2.53) we end up with

$$\partial_r^2\tilde{n}_\ell(kr) + \left[1 - \frac{2\ell}{kr}\partial_r\right]\tilde{n}_\ell(kr) = 0. \tag{2.57}$$

The terms

$$\frac{2\ell}{kr}$$

and

$$\frac{2\ell}{(kr)^2}$$

from (2.56) and (2.57) are analytic, therefore from the theorem we may conclude that $\tilde{j}_\ell(kr)$ and $\tilde{n}_\ell(kr)$ are analytic functions of the parameter ℓ. As a result $j_\ell(kr)$ and $n_\ell(kr)$ are analytical, because the product analytic functions it is also analytic. As a consequence $h_\ell^{(\pm)}(kr)$ is analytic, since a linear combination of analytic functions it is also analytic.

Since the coefficients in Eqs. (2.15)-(2.16) are analytic functions of the parameter ℓ, and the boundary conditions (2.19) do not depend on ℓ, according to the Poincarè theorem the functions $F_\ell^{(in/out)}(E,r)$ are analytic in the ℓ-plane. Thus, the unknown functions, $F_\ell^{(in/out)}(E,r)$, and the Riccati-Hankel functions, $h_\ell^{(\pm)}(kr)$, can be expressed as a power series:

$$h_\ell^{(\pm)}(kr) = \sum_{n=0}^{\infty}(\ell-\ell_0)^n X_n^{(\pm)}(k,r,\ell_0), \tag{2.58}$$

$$F_\ell^{(in/out)}(E,r) = \sum_{n=0}^{\infty}(\ell-\ell_0)^n \varphi_n^{(in/out)}(E,r), \tag{2.59}$$

where $\varphi_n^{(in/out)}(E,r)$ are unknown expansion coefficients and

$$X_n^{(\pm)}(k,r,\ell_0) = \frac{1}{n!}\partial_\ell^n h_l^{(\pm)}(kr)|_{\ell=\ell_0}, \tag{2.60}$$

ℓ_0 is the center of expansion. The derivatives (2.60) cannot be found analytically. We therefore have to calculate them numerically. A stable procedure that we will use for calculations is given in Appendix B.

From Eqs. (2.21)-(2.22), we conclude that the power series of the Jost functions is given by

$$f_\ell^{(in/out)}(E) = \sum_{n=0}^{\infty}(\ell-\ell_0)^n \lim_{r\to\infty} \varphi_n^{(in/out)}(E,r,\ell_0). \tag{2.61}$$

2.4 Linear independence at the complex momentum

As discussed in section 2.1.1 on page 8, the solutions of the differential equation (2.41) must be linearly independent, but if

$$Re(\ell) = -\frac{1}{2},$$

and as $r \longrightarrow 0$:

$$j_\ell(kr) \longrightarrow (kr)^{\ell+1} = (kr)^{\frac{1}{2}} \tag{2.62}$$

$$n_\ell(kr) \longrightarrow (kr)^{-\ell} = (kr)^{\frac{1}{2}} \tag{2.63}$$

equations (2.62) and (2.63) become linearly dependent. Therefore we will only consider angular momentum of the form

$$\mathrm{Re}(\ell) > -\frac{1}{2}. \tag{2.64}$$

2.5 Power series of the Jost function

In section 2.1, we derivated a method for calculating the Jost functions as well as defining a power series. And in section 2.2, we showed that the Regge poles for scattering states are located in the first quadrant of the complex ℓ-plane. Finally, we have shown in section 2.3 that, if an arbitrary circle with center ℓ_0 is chosen on the first quadrant of the complex ℓ-plane, the Jost functions will be analytic within that circle. Moreover, we have shown that the power series expansion of the Jost functions within a circle is given by (2.61). The only thing that is left, is to determine expansion coefficients. Thus, this will be the main focus of this section.

In order for us to obtain the expansion coefficients of the power series (2.61), we start but substituting the expansions (2.58)-(2.59) into (2.15) and obtain:

$$\begin{aligned}\sum_{n=0}^{\infty}(\ell-\ell_0)^n\partial_r\varphi_n^{(in)} = -\frac{V(r)}{2ik}\sum_{\alpha=0}^{\infty}(\ell-\ell_0)^\alpha X_\alpha^{(+)}\left[\sum_{\beta=0}^{\infty}(\ell-\ell_0)^\beta X_\beta^{(-)}\right.\\ \left.\times\sum_{\gamma=0}^{\infty}(\ell-\ell_0)^\gamma\varphi_\gamma^{(in)} + \sum_{\beta'=0}^{\infty}(\ell-\ell_0)^{\beta'}X_{\beta'}^{(+)}\sum_{\gamma'=0}^{\infty}(\ell-\ell_0)^{\gamma'}\varphi_{\gamma'}^{(out)}\right].\end{aligned} \tag{2.65}$$

We now expand the LHS of (2.65)

$$\sum_{n=0}^{\infty}(\ell-\ell_0)^n\partial_r\varphi_n^{(in)} = \partial_r\varphi_0^{(in)} + (\ell-\ell_0)\partial_r\varphi_1^{(in)} + (\ell-\ell_0)^2\partial_r\varphi_2^{(in)} + \ldots \tag{2.66}$$

and the RHS, without the $-V(r)/2ik$ term

$$\left(X_0^{(+)}+(\ell-\ell_0)X_1^{(+)}+(\ell-\ell_0)^2X_2^{(+)}+...\right)\left[X_0^{(-)}\varphi_0^{(in)}+X_0^{(+)}\varphi_0^{(out)}\right.$$
$$(\ell-\ell_0)\left(X_0^{(-)}\varphi_1^{(in)}+X_1^{(-)}\varphi_0^{(in)}+X_0^{(+)}\varphi_1^{(out)}+X_1^{(+)}\varphi_0^{(out)}\right)$$
$$+(\ell-\ell_0)^2\left(X_0^{(-)}\varphi_2^{(in)}+X_1^{(-)}\varphi_1^{(in)}+X_2^{(-)}\varphi_0^{(in)}+X_0^{(+)}\varphi_2^{(out)}+X_1^{(+)}\varphi_1^{(out)}\right.$$
$$\left.+X_2^{(+)}\varphi_0^{(out)}\right)+(\ell-\ell_0)^3\left(X_1^{(-)}\varphi_2^{(in)}+X_2^{(-)}\varphi_1^{(in)}+X_1^{(-)}\varphi_2^{(out)}\right.$$
$$\left.\left.+X_2^{(+)}\varphi_1^{(out)}\right)+...\right] \tag{2.67}$$

simplifying (2.67)

$$X_0^{(+)}\left(X_0^{(-)}f_0^{(in)}+X_0^{(+)}f_0^{(out)}\right)+(\ell-\ell_0)\left[X_0^{(+)}\left(X_0^{(-)}\varphi_1^{(in)}+X_0^{(+)}\varphi_1^{(out)}\right)\right.$$
$$+X_0^{(+)}\left(X_1^{(-)}\varphi_0^{(in)}+X_1^{(+)}\varphi_0^{(out)}\right)+X_1^{(+)}\left(X_0^{(-)}\varphi_0^{(in)}+X_0^{(+)}\varphi_0^{(out)}\right)\Big]$$
$$+(\ell-\ell_0)^2\left[X_0^{(+)}\left(X_0^{(-)}\varphi_2^{(in)}+X_0^{(+)}\varphi_2^{(out)}\right)+X_0^{(+)}\left(X_1^{(-)}\varphi_1^{(in)}+X_1^{(+)}\varphi_1^{(out)}\right)\right.$$
$$+X_0^{(+)}\left(X_2^{(-)}\varphi_0^{(in)}+X_2^{(+)}\varphi_0^{(out)}\right)+X_1^{(+)}\left(X_0^{(-)}\varphi_1^{(in)}+X_0^{(+)}\varphi_1^{(out)}\right)$$
$$\left.+X_1^{(+)}\left(X_1^{(-)}\varphi_0^{(in)}+X_1^{(+)}\varphi_0^{(out)}\right)+X_2^{(+)}\left(X_0^{(-)}\varphi_0^{(in)}+X_0^{(+)}\varphi_0^{(out)}\right)\right]+... \tag{2.68}$$

The next step is to equate the coefficients of $(\ell-\ell_0)$ with the same exponent, from (2.66) and (2.68), it follows that
$(\ell-\ell_0)^0$:

$$\partial_r\varphi_0^{(in)}=-\frac{V}{2ik}X_0^{(+)}\left(X_0^{(-)}\varphi_0^{(in)}+X_0^{(+)}\varphi_0^{(out)}\right)$$

$(\ell - \ell_0)^1$:

$$\begin{aligned}\partial_r \varphi_1^{(in)} = &-\frac{V}{2ik} X_0^{(+)} \left(X_0^{(-)} \varphi_1^{(in)} + X_0^{(+)} \varphi_1^{(out)} \right) \\ &- \frac{V}{2ik} X_0^{(+)} \left(X_1^{(-)} \varphi_0^{(in)} + X_1^{(+)} \varphi_0^{(out)} \right) \\ &- \frac{V}{2ik} X_1^{(+)} (X_0^{(-)} \varphi_0^{(in)} + X_0^{(+)} \varphi_0^{(out)} \Big) ,\end{aligned} \tag{2.69}$$

$(\ell - \ell_0)^2$:

$$\begin{aligned}&\partial_r \varphi_2^{(in)} = -\frac{V}{2ik} X_0^{(+)} \left(X_0^{(-)} \varphi_2^{(in)} + X_0^{(+)} \varphi_2^{(out)} \right) \\ &- \frac{V}{2ik} X_0^{(+)} \left(X_1^{(-)} \varphi_1^{(in)} + X_1^{(+)} \varphi_1^{(out)} \right) - \frac{V}{2ik} X_0^{(+)} \left(X_2^{(-)} \varphi_0^{(in)} + X_2^{(+)} \varphi_0^{(out)} \right) \\ &- \frac{V}{2ik} X_1^{(+)} \left(X_0^{(-)} \varphi_1^{(in)} + X_0^{(+)} \varphi_1^{(out)} \right) - \frac{V}{2ik} X_1^{(+)} \left(X_1^{(-)} \varphi_0^{(in)} + X_1^{(+)} \varphi_0^{(out)} \right) \\ &- \frac{V}{2ik} X_2^{(+)} \left(X_0^{(-)} \varphi_0^{(in)} + X_0^{(+)} \varphi_0^{(out)} \right) .\end{aligned} \tag{2.70}$$

Therefore the general expression for the expansion coefficients of Eq. (2.61) becomes

$$\partial_r \varphi_n^{(in)} = -\frac{V}{2ik} \sum_{\alpha+\beta+\gamma=n} X_\alpha^{(+)} \left[X_\beta^{(-)} \varphi_\gamma^{(in)} + X_\beta^{(+)} \varphi_\gamma^{(out)} \right] . \tag{2.71}$$

Similiarly, we obtain

$$\partial_r \varphi_n^{(out)} = \frac{V}{2ik} \sum_{\alpha+\beta+\gamma=n} X_\alpha^{(-)} \left[X_\beta^{(-)} \varphi_\gamma^{(in)} + X_\beta^{(+)} \varphi_\gamma^{(out)} \right] , \tag{2.72}$$

where the $X_{\alpha/\beta}^{(\pm)}$ are defined as in (2.60). The boundary condition that will

be used to solve (2.71) and (2.72):

$$F_\ell^{(in/out)}(E,0) = \sum_{n=0}^{\infty}(\ell-\ell_0)^n\varphi_n^{(in/out)}(E,0)$$
$$= \varphi_0^{(in/out)}(E,0) + (\ell-\ell_0)\varphi_1^{(in/out)}(E,0) + (\ell-\ell_0)^2\varphi_2^{(in/out)}(E,0) + ... \tag{2.73}$$

According to Eq.(2.19) on page 11, the LHS of (2.73) is ℓ-independent. This implies that the RHS should have the same independence. Therefore all the $\varphi_i^{(in/out)}$'s whose coefficient depends on ℓ should be zero. It follows that

$$\varphi_n^{(in/out)}(E,0) = \delta_{n0}. \tag{2.74}$$

Eq. (2.74) is the boundary condition that will be used to solve the differential equations (2.71)-(2.72).

Chapter 3

Differential cross-sectional area

In chapter 2, we obtained a power series expansion of the Jost function in the complex ℓ-plane and also proposed a method for calculating the expansion coefficients of the power series. In this chapter, we will define scattering amplitude and relate it with the power series of the Jost functions, moreover we will make use of the Watson transformation to express the scattering amplitude as a sum of the background and pole term. Furthermore, we demostrate the application of this approach, by applying it to the Born approximation and determine its effects.

3.1 Scattering amplitude

Quantum scattering is a transformation of the incoming wave into scattered wave at real positive energies. The scattering cross section, which is a fraction of the incident area that is scattered by a potential into a solid angle, is obtained by squaring the scattering amplitude. The subsequent sections are devoted to deriving an expression for calculating the scattering amplitude, which will enable us to determine scattering cross section.

The scattering wave function, as $r \to \infty$, is given by

$$\psi_{\mathbf{k}}(\mathbf{r}) = \frac{1}{(2\pi)^{2/3}} \left[e^{\mathbf{kr}} + \frac{e^{kr}}{r} f_{\mathbf{k}}(\hat{\mathbf{r}}) \right], \qquad r \to \infty. \tag{3.1}$$

The first term in (3.1) represents the incident plane wave with momentum $\mathbf{k}$ (in the direction of the incident plane), while the second term represents the outgoing wave scattered spherically in all directions with the amplitude $f_{\mathbf{k}}(\hat{\mathbf{r}})$.

The differential scattering cross section is defined as

$$\frac{d\sigma}{d\Omega} = |f_{\mathbf{k}}(\hat{\mathbf{r}})|^2, \tag{3.2}$$

in which the LHS of (3.2) represents the fraction of the incoming flux cross-section, $d\sigma$, scattered into the solid angle, $d\Omega$, in the $\hat{\mathbf{r}}$ direction. For spherical symmetrical potentials, the scattering amplitude will be ϕ-independent, thus can be expanded using Legendre polynomials

$$f_{\mathbf{k}}(\hat{\mathbf{r}}) = \sum_{\ell=0}^{\infty} (2\ell + 1) f_\ell(E) P_\ell(\cos\theta). \tag{3.3}$$

The expression (3.3) is known as the partial wave expansion. As it was stated in the introduction, it is most useful when the potential is of finite range and only there is a small number of partial waves that contribute to the scattering amplitude, in other words, the orbital angular momentum should at most be Rk i.e

$$\ell \leq kR,$$

where k and R are the momentum of the plane wave and range of the potential, respectively. In Eq. (3.3), $\mathbf{k}$ is the incident momentum, θ the angle between $\mathbf{k}$ and $\hat{\mathbf{r}}$ which is the scattering angle and $P_\ell(\cos\theta)$ is the Legendre

polynomial of degree ℓ. The partial wave amplitude is

$$f_\ell(E) = \frac{S_\ell(E) - 1}{2ik} = \frac{1}{2ik}\left[\frac{f_\ell^{(out)}(E)}{f_\ell^{(in)}(E)} - 1\right] = \frac{e^{i\delta_\ell(E)}\sin\delta_\ell(E)}{k}. \tag{3.4}$$

The real function $\delta_\ell(E)$ is called the phase shift.

3.1.1 Scattering amplitude at low energies

We now investigate the behavior of (3.3) when $k \to 0$. We start by integrating the LHS and RHS of equations (2.15) - (2.16) and impose the boundary condition (2.19), we obtain

$$\begin{aligned} F_\ell^{(in)}(E,r) &= 1 - \frac{1}{2ik}\int_0^r h_\ell^{(+)}(kr')V(r')u_\ell(E,r')\,dr' \\ F_\ell^{(out)}(E,r) &= 1 + \frac{1}{2ik}\int_0^r h_\ell^{(-)}(kr')V(r')u_\ell(E,r')\,dr', \end{aligned} \tag{3.5}$$

where

$$u_\ell(E,r) = h_\ell^{(-)}(kr')F_\ell^{(in)}(E,r') + h_\ell^{(+)}(kr')F_\ell^{(out)}(E,r'),$$

represents the radial wave function. We solve (3.5) for $u_\ell(E,r)$ by multiplying $F_\ell^{(in)}(E,r)$ and $F_\ell^{(out)}(E,r)$ by $h_\ell^{(-)}(kr)$ and $h_\ell^{(+)}(kr)$, respectively, then summing up the product together

$$u_\ell(E,r) = h_\ell^{(-)}(kr)F_\ell^{(in)}(E,r) + h_\ell^{(+)}(kr)F_\ell^{(out)}(E,r)$$

$$= h_\ell^{(+)}(kr) + h_\ell^{(-)}(kr) + \frac{1}{2ik}\int_0^r \left[h_\ell^{(+)}(kr)h_\ell^{(-)}(kr') - h_\ell^{(-)}(kr)h_\ell^{(+)}(kr')\right] V(r')u_\ell(E,r')\,dr'$$

$$= 2j_\ell(kr) + \frac{1}{ik}\int_0^r \left[h_\ell^{(+)}(kr)j_\ell(kr') - j_\ell(kr)h_\ell^{(+)}(kr')\right] V(r')u_\ell(E,r')\,dr'$$

$$= 2j_\ell(kr) + \int_0^r g(r,r',k)V(r')u_\ell(E,r')$$

$$\therefore u_\ell(E,r) = 2j_\ell(kr) + \int_0^r g(r,r',k)V(r')u_\ell(E,r')\,dr'. \tag{3.6}$$

With the Green's function defined as

$$g(r,r',k) = \frac{1}{ik}\left[h_\ell^{(+)}(kr)j_\ell(kr') - j_\ell(kr)h_\ell^{(+)}(kr')\right].$$

As $k \to 0$,

$$j_\ell(kr)h_\ell^{(+)}(kr') \quad \underset{k\to 0}{\longrightarrow} \quad \frac{(kr)^{\ell+1}}{1\cdot 3\cdot 5\cdots(2\ell+1)} \times \left[-i\frac{1\cdot 3\cdot 5\cdots(2\ell-1)}{(kr')^\ell}\right]$$
$$= \frac{ik(2\ell-1)r^{\ell+1}}{(2\ell+1)(r')^\ell}$$
$$j_\ell(kr')h_\ell^{(+)}(kr') \quad \underset{k\to 0}{\longrightarrow} \quad \frac{ik(2\ell-1)(r')^{\ell+1}}{(2\ell+1)r^\ell}$$

$$\therefore g(r,r') \quad \underset{k\to 0}{\longrightarrow} \quad \frac{2\ell-1}{2\ell+1}\left[\frac{(r')^{\ell+1}}{r^\ell} - \frac{r^{\ell+1}}{(r')^\ell}\right]. \tag{3.7}$$

Eq. (3.7) suggests that for low energies the Green's function does not depend

on the momentum. As a result, the radial wave function, $u_\ell(E,r)$ will have the same k-dependence as $j_\ell(kr)$, which is $k^{\ell+1}$. The integration equation for the partial wave amplitude, for finite range potentials, is given by [10],

$$\begin{aligned} f_\ell(k) &= -\frac{1}{k^2}\int_0^r j_\ell(kr')U(r')u_\ell(E,r')\,dr' \\ &\xrightarrow[k\to 0]{} -\frac{1}{k^2}\int_0^r \frac{(kr')^{\ell+1}}{1\cdot 3\cdot 5\cdots(2\ell+1)}U(r')\frac{(kr')^{\ell+1}}{1\cdot 3\cdot 5\cdots(2\ell+1)}\,dr' \\ &= -\frac{1}{k^2}\int_0^r U(r')\frac{(kr')^{2\ell+2}}{(1\cdot 3\cdot 5\cdots(2\ell+1))^2}\,dr' \\ &= \frac{k^{2\ell}}{(1\cdot 3\cdot 5\cdots(2\ell+1))^2}\int_0^r (r')^{2\ell+2}U(r')\,dr'. \end{aligned}$$

Thus

$$f_\ell(k) \xrightarrow[k\to 0]{} k^{2\ell}\alpha_\ell(r), \tag{3.8}$$

where

$$\alpha_\ell(r) = \int_0^r \frac{(r')^{2\ell+2}U(r')}{(1\cdot 3\cdot 5\cdots(2\ell+1))^2}\,dr'.$$

Substituting (3.8) into (3.3):

$$\begin{aligned} f_{\mathbf{k}}(\hat{\mathbf{r}}) &= \sum_{\ell=0}^{\infty}(2\ell+1)f_\ell(E)P_\ell(\cos\theta) \\ &= f_0P_0(1) + 3f_1P_1(1) + 5f_2P_2(1) + 7f_3P_3(1) + ... \\ &\xrightarrow[k\to 0]{} -\alpha_0 - 3\alpha_1k^2P_1(1) - 5\alpha_2k^4P_2(1) - ... \\ &= -\alpha_0 \end{aligned} \tag{3.9}$$

In Eq. (3.9) we have showed that for low energies, $k \to 0$, the scattering

amplitude converges to a single term , $\alpha_0(r)$. But once the energy increases more terms in the series will be required.

3.1.2 Properties of $\delta_\ell(E)$

For large angular momentum, $\ell \to \infty$, and fixed k, the centrifugal barrier $\ell(\ell+1)/r^2$ in the Schrödinger equation (2.1) on page 8 will dominate the potential (finite range), as a result, the outgoing wave will be slightly distorted and therefore $\delta_\ell(E) \to 0$. On the other hand, if we fix ℓ and allow momentum to take large values, $k \to \infty$, the momentum term in (2.1) will dominate both the potential and potential barrier. This implies that the solution of the Schröndger equation will be that of the 'free' wave function, experiencing no potential, therefore $\delta_\ell(E) \to 0$. Hence, the phase shift approaches zero when both ℓ and k goes to infinity.

We will use these properties in section 3.2 to prove that the scattering amplitude approaches zero as $\ell \to \infty$.

3.2 Watson transformation

As the energy increases more terms are required, as a result (3.3) will converge slowly. This difficulty with convergence can be avoided by allowing the variable ℓ to take on complex values. For complex values of angular momentum ℓ, the infinite sum in (3.3) can be converted to a convergent integral using the Watson transformation. In order for us to perform this transformation, let us consider the following contour integral

$$I = \oint_C \frac{(2\lambda+1) f_\lambda(E) P_\lambda(-\cos\theta)}{\sin(\pi\lambda)}\, d\lambda, \tag{3.10}$$

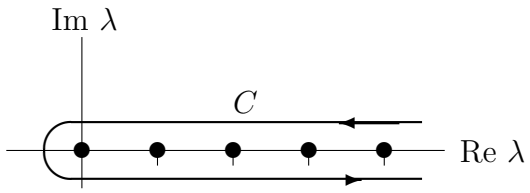

Figure 3.1: The integration contour C, used in eq (3.17), which encloses all the non-negative integer values of λ.

where λ is a complex variable and the integration path, C, encloses all the non-negative integer values of λ, in a counter-clockwise direction, as shown in Fig. (3.1). $P_\lambda(-\cos\theta)$ is no longer a Legendre polynomial rather its a Legendre function of complex degree λ. The poles of the integrand are located at

$$\sin(\pi\lambda)|_{\lambda=\ell} = 0 \quad \text{for} \quad \ell = 0, 1, 2, 3... \tag{3.11}$$

Eq. (3.11) shows that we have first ordered poles. From the residue theorem [11], Eq. (3.10) may be written as

$$I = 2\pi i \sum_{\ell=0}^{\infty} \text{Res}\left[\frac{(2\lambda+1) f_\lambda(E) P_\lambda(-\cos\theta)}{\sin(\pi\lambda)}, \ell\right]. \tag{3.12}$$

The expression $Res[f(z), z_0]$ stands for the residue of the function $f(z)$ at the point z_0. Since the poles are of first order the residue term in (3.12) is calculated as

$$\begin{aligned}\text{Res}\left[\frac{(2\lambda+1) f_\lambda(E) P_\lambda(-\cos\theta)}{\sin(\pi\lambda)}, \ell\right] &= \lim_{\lambda\to\ell}(\lambda-\ell)\left[\frac{(2\lambda+1) f_\lambda(E) P_\lambda(-\cos\theta)}{\sin(\pi\lambda)}\right] \\ &= (2\ell+1) f_\ell(E) P_\ell(-\cos\theta) \lim_{\lambda\to\ell}\left(\frac{\lambda-\ell}{\sin(\pi\lambda)}\right).\end{aligned} \tag{3.13}$$

$\lim_{\lambda\to\ell}\left(\frac{\lambda-\ell}{\sin(\pi\lambda)}\right)$ has the form $\frac{0}{0}$. This limit can be evaluated using the l'Hôpital's rule,

$$\lim_{\lambda\to\ell}\left(\frac{\lambda-\ell}{\sin(\pi\lambda)}\right) = \lim_{\lambda\to\ell}\frac{\frac{\mathrm{d}}{\mathrm{d}\lambda}(\lambda-\ell)}{\frac{\mathrm{d}}{\mathrm{d}\lambda}(\sin(\pi\lambda))} = \frac{1}{(-1)^\ell\pi}. \tag{3.14}$$

Substituting (3.13)-(3.14) into (3.12) and equate the result to (3.10):

$$\oint \frac{(2\lambda+1)f_\lambda(E)P_\lambda(-\cos\theta)}{\sin(\pi\lambda)}\,d\lambda = 2i\sum_{\ell=0}^{\infty}\frac{(2\ell+1)f_\ell(E)P_\ell(-\cos\theta)}{(-1)^\ell} \tag{3.15}$$

Using the identity $P_\ell(-x) = (-1)^\ell P_\ell(x)$, we end up with

$$\sum_{\ell=0}^{\infty}(2\ell+1)f_\ell(E)P_\ell(\cos\theta) = \frac{1}{2i}\oint_C \frac{(2\lambda+1)f_\lambda(E)P_\lambda(-\cos\theta)}{\sin(\pi\lambda)}\,d\lambda. \tag{3.16}$$

We have successfully converted the slow converging infinite sum on the left hand side into an integral on the right hand side. Eq. (3.16) is known as the Watson transformation. Comparing (3.3) with (3.16) we obtain

$$f_{\mathbf{k}}(\hat{\mathbf{r}}) = \frac{1}{2i}\oint_C \frac{(2\lambda+1)f_\lambda(E)P_\lambda(-\cos\theta)}{\sin(\pi\lambda)}\,d\lambda. \tag{3.17}$$

The RHS of (3.17) has two important properties:

1. The integrand is a meromorphic function of λ i.e it is analytic everywhere except at isolated poles. This means that the integration contour, C, can be arbitrary deformed under the condition that it does not cross any singularities (poles).

2. The amplitude, $|f_\ell(E)|$, tends to zero when $\ell \to \infty$ on the complex ℓ-plane. This implies that we can ignore any parts of the deformed contour that are at infinity.

Below will we provide a proof of statement 2, but before that we state an important remark. If the projectile particle does not experience the scattering potential i.e it moves freely, the scattering phase shift will be zero, whereas, if a potential is present, the phase shift will not be zero. From this we can conclude that, if the incident plane wave experiences weak potential,

the phase shift will approach zero.

Reference [1], [10] and the properties of $\delta_\ell(E)$ on page 32 suggest that as $\ell \to \infty$, the centrifugal potential, $\ell(\ell+1)/2mr^2$ - from the Schrödinger, tends to repel the particles away from the actual potential, $V(r)$, becomes more repulsive. Since our potential is finite this implies that the probability that the incident particle will experience the potential $V(r)$ is small, hence the scattering phase shift, $\delta_\ell(E)$, will approach zero. Then it follows from (3.4) that:

$$|f_\ell(E)| = \frac{1}{p}\,|\sin\delta_\ell(E)| \leq \frac{1}{p}\,|\delta_\ell(E)| \to 0. \tag{3.18}$$

In (3.18) we have used the property that

$$|\sin x| \leq |x| \quad \text{for} \quad x \to 0.$$

We thus obtain

$$|f_\ell(E)| \underset{\ell\to\infty}{\longrightarrow} 0. \tag{3.19}$$

Eq. (3.19) implies that only a finite number of terms will be required to approximate the scattering amplitude (3.3). This supports the assertion that was made on section 3.1 on page 28 that the maximum number of terms that contributes to the scattering amplitude is

$$\ell \leq kR.$$

3.2.1 Properties of the S-matrix

According to Tamara and Holterner [7], The S-matrix, for finite range potentials has the following asymptotic behaviour:

$$|S_\lambda(E)| \underset{|\lambda|\to\infty}{\longrightarrow} \begin{cases} 0, & \text{for } \operatorname{Im}\lambda \geq 0 \\ \infty, & \text{for } \operatorname{Im}\lambda < 0 \end{cases} \tag{3.20}$$

They further said that, the scattering amplitude may be represented as a sum of the pole and background terms. The background integral must run from positive infinity along the imaginary angular momentum axis and instead of continuing towards negative infinity along the imaginary axis, it must be bent such that $\operatorname{Re}\ell \to \infty$, in order to satisfy (3.20).

As the contour C moves away from the $\operatorname{Re}\lambda$ axis towards positive $\operatorname{Im}\lambda$ axis, it picks up a finite number of poles. Since the contour cannot pass through the poles, it will form loops around each pole as shown in Fig. (3.2a). The paths of b_1 and b_2 move in opposite directions, as the distance between them approaches zero, the two paths will cancel one another and hence form Fig. (3.2b). This cancellation enables us to move from Fig. (3.2b) to Fig. (3.2c). If we widen the contour in Fig.(3.2c) we obtain C_2 in Fig.(3.2d).

The first property of the scattering amplitude on page 34 and (3.20) allows us to deform the contour C into C_1 and C_2 as shown in Fig. (3.2), where C_1 runs down the imaginary axis from $+i\infty$ curve's around the pole $\lambda = 0$ on the negative real axis then goes to infinity - parallel to the $\operatorname{Re}\lambda$ axis. C_2 encloses all the Regge poles, in a clockwise direction and C_1 forms the background integral.

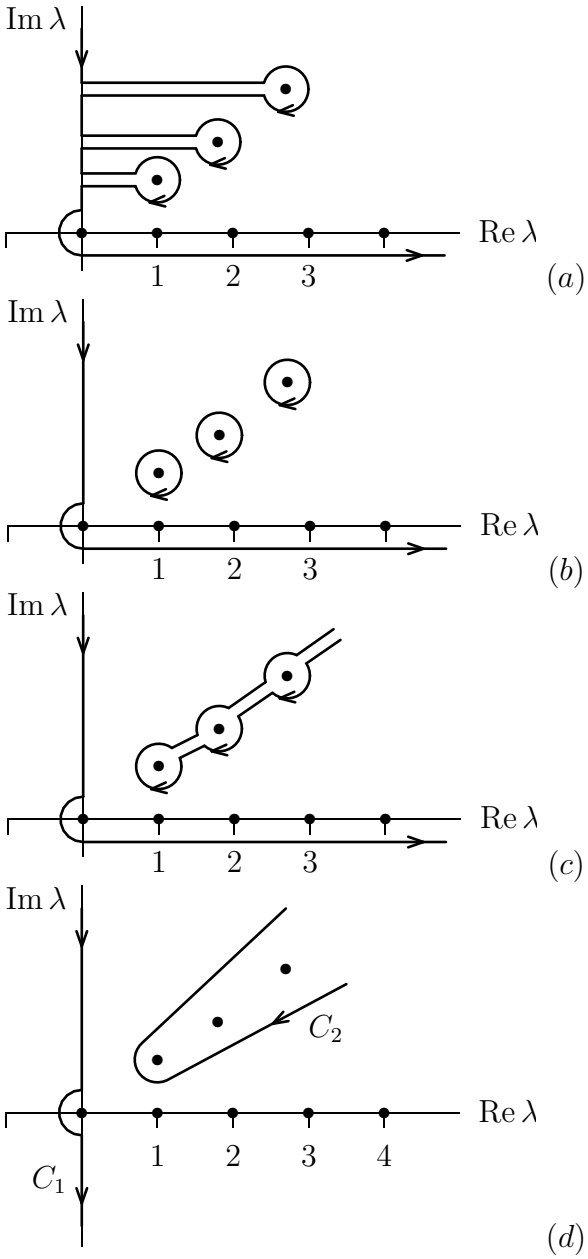

Figure 3.2: The steps to deform the integration contour shown in Fig. 3. These steps replace the initial contour C with the two contours C_1 and C_2

.

The scattering amplitude for the deformed contour C becomes

$$f_{\vec{k}}(\hat{\vec{r}}) = f_{\vec{k}}^{(bg)}(\hat{\vec{r}}) + f_{\vec{k}}^{(p)}(\hat{\vec{r}}). \tag{3.21}$$

The superscripts (bg) and (p) represents the background and pole contributions, respectively, where

$$f_{\vec{k}}^{(bg)}(\hat{\vec{r}}) = \frac{1}{2i}\int_{C_1} \frac{(2\lambda+1)f_\lambda(E)P_\lambda(-\cos\theta)}{\sin[\pi(\lambda-\epsilon)]}\, d\lambda, \tag{3.22}$$

and

$$\begin{aligned} f_{\vec{k}}^{(p)}(\hat{\vec{r}}) &= \frac{1}{2i}\oint_{C_2} \frac{(2\lambda+1)f_\lambda(E)P_\lambda(-\cos\theta)}{\sin(\pi\lambda)}\, d\lambda \\ &= -\pi\sum_n \frac{2\ell_n+1}{\sin(\pi\ell_n)} P_{\ell_n}(-\cos(\theta)) Res[f_\lambda(E),\ell_n], \end{aligned} \tag{3.23}$$

where ℓ_n is the n^{th} Regge pole and the negative sign is due to the clockwise motion of contour C_2.

3.3 Evaluation of the pole term

For us to calculate the scattering amplitude in (3.21), we have to evaluate the residue term in Eq. (3.23),

$$\begin{aligned} \text{Res}[f_\ell(E),\ell_n] &= \lim_{\ell\to\ell_n}(\ell-\ell_n)f_\ell(E) = \frac{1}{2ik}\lim_{\ell\to\ell_n}(\ell-\ell_n)\left[\frac{f_\ell^{(out)}(E)}{f_\ell^{(in)}(E)} - 1\right] \\ &= \frac{1}{2ik}\lim_{\ell\to\ell_n}(\ell-\ell_n)\left[\frac{f_\ell^{(out)}(E)}{f_\ell^{(in)}(E)}\right], \end{aligned} \tag{3.24}$$

substituting (2.61) into (3.24)

$$\mathrm{Res}[f_\ell(E),\ell_n]=\frac{1}{2ik}\lim_{\ell\to\ell_n}(\ell-\ell_n)\frac{\varphi_0^{(out)}+(\ell-\ell_n)\varphi_1^{(out)}+...}{\varphi_0^{(in)}+(\ell-\ell_n)\varphi_1^{(in)}+...}. \tag{3.25}$$

At each ℓ_n, there is a first-order pole of the S-matrix, which means that

$$\varphi_0^{(in)}=0. \tag{3.26}$$

Then (3.25) becomes:

$$\mathrm{Res}[f_\ell(E),\ell_n]=\frac{1}{2ik}\frac{\varphi_0^{(out)}(E,\ell_n)}{\varphi_1^{(in)}(E,\ell_n)}. \tag{3.27}$$

We evaluate (3.27) by solving the following systems of linear differential equations for $\varphi_1^{(in)}$ and $\varphi_0^{(out)}$:

$$\varphi_0^{'(in)}(E,r,\ell_n)=-\frac{V}{2ik}X_0^{(+)}\left(X_0^{(-)}\varphi_0^{(in)}+X_0^{(+)}\varphi_0^{(out)}\right), \tag{3.28}$$

$$\varphi_0^{'(out)}(E,r,\ell_n)=\frac{V}{2ik}X_0^{(-)}\left(X_0^{(-)}\varphi_0^{(in)}+X_0^{(+)}\varphi_0^{(out)}\right), \tag{3.29}$$

$$\begin{aligned}\varphi_1^{'(in)}(E,r,\ell_n)=-\frac{V}{2ik}\Big(&X_0^{(+)}\left(X_0^{(-)}\varphi_1^{(in)}+X_0^{(+)}\varphi_1^{(out)}+X_1^{(-)}\varphi_0^{(in)}\right.\\&\left.+X_1^{(+)}\varphi_0^{(out)}+X_1^{(+)}\left(X_0^{(-)}\varphi_0^{(in)}+X_0^{(+)}\varphi_0^{(out)}\right)\right),\end{aligned} \tag{3.30}$$

$$\begin{aligned}\varphi_1^{'(out)}(E,r,\ell_n)=\frac{V}{2ik}\Big(&X_0^{(-)}\left(X_0^{(-)}\varphi_1^{(in)}+X_0^{(+)}\varphi_1^{(out)}+X_1^{(-)}\varphi_0^{(in)}\right.\\&\left.+X_1^{(+)}\varphi_0^{(out)}+X_1^{(-)}\left(X_0^{(-)}\varphi_0^{(in)}+X_0^{(+)}\varphi_0^{(out)}\right)\right).\end{aligned} \tag{3.31}$$

The Legendre function for complex λ is obtained by solving the differential equation [12]

$$(1-z^2)\frac{d^2P_\lambda(z)}{dz^2} - 2z\frac{dP_\lambda(z)}{dz} + \lambda\left(\lambda+1\right)P_\lambda(z) = 0, \tag{3.32}$$

with boundary conditions

$$\left[\frac{dP_\lambda(z)}{dz}\right]_{z=0} = \frac{2}{\sqrt{\pi}}\sin\left(\frac{\lambda\pi}{2}\right)\frac{\Gamma\left(\lambda/2+1\right)}{\Gamma(\lambda/2+1/2)} \tag{3.33}$$

$$P_\lambda(0) = \pi^{-\frac{1}{2}}\cos\left(\frac{\lambda\pi}{2}\right)\frac{\Gamma\left(\lambda/2+1\right)}{\Gamma(\lambda/2+1/2)}. \tag{3.34}$$

We have shown that for us to calculate numerically the pole term (3.23), we must calculate the expansion coefficients of the power series (2.61) by numerically solving (2.71) and (2.72). Therefore, the pole term explicitly depends on the expansion coefficients of the power series expansion of the Jost functions.

Chapter 4

Application

The method that we have developed thus far, expresses the scattering amplitude as a sum of the background term and pole term. Futhermore, this method proposes a procedure that should be used for calculating the pole term but it doesn't tell us anyhting about the background term. To demostrate how this method may be used in application, we will let the background term to be equal to the Born approximation. As a result, we will now focus on deriving an expression for the Born approximation.

4.1 Born Approximation

For weak potentials, the incoming plane wave will be deflected only by a small amount, i.e the scattering angle will be small. Moreover, small scattering angles are also a result of plane waves that are incident at high energies. For this scenario, the scattered wave (outgoing wave) may be approximated by the incident plane wave - this approximation is called the first Born Approximation, which we shall refer to as the Born approximation.

The scattering amplitude for the Born approximation is expressed as [1]:

$$f(\theta,\phi) = -\frac{\mu}{2\pi\hbar}\int_0^\infty e^{i\vec{q}\cdot\vec{r}}V(\vec{r})\,d^3r, \tag{4.1}$$

where $\vec{q} = \vec{k'} - \vec{k}$ is the momentum transfer, $\vec{k'}$ and $\vec{k}$ are the outgoing and incoming momenta, respectively. We will only consider elastic scattering, i.e momentum before equals momentum after. As a result, the magnitude of $\vec{k'}$ is equal to that of $\vec{k}$, given this, the momentum transfer is defined as:

$$q = |\vec{k'} - \vec{k}| = \sqrt{k'^2 - 2\vec{k'}\cdot\vec{k} + k^2} = k\sqrt{2(1-\cos\theta)}, \tag{4.2}$$

under the square root we have

$$\begin{aligned} 2(1-\cos\theta) &= 2(1-\cos^2(\theta/2)+\sin^2(\theta/2)) \\ &= 2(1-1+2\sin^2(\theta/2)) \\ &= 4\sin^2(\theta/2). \end{aligned}$$

Therefore (4.2)

$$q = 2k\sin(\theta/2). \tag{4.3}$$

For short-range spherical symmetric potentials, $V(\vec{r}) = V(r)$, using spherical coordinates in (4.1) we obtain

$$\begin{aligned}\int_0^\infty e^{i\vec{q}\cdot\vec{r}}V(\vec{r})\,d^3r &= \int_0^\infty r^2V(r)\,dr\int_0^\pi e^{iqr\cos\theta}\sin\theta\,d\theta\int_0^{2\pi}d\phi \\ &= 2\pi\int_0^\infty r^2V(r)\,dr\int_{-1}^{1}e^{iqrx}\,dx \\ &\quad \text{we let } x=\cos\theta \Rightarrow\ dx=\sin\theta\,d\theta \\ &\quad \text{and let } e^{ip}=\cos p+i\sin p \\ &= \frac{4\pi}{q}\int_0^\infty r^2V(r)\sin(qr)\,dr.\end{aligned} \tag{4.4}$$

Substituting (4.4) and (4.3) into (4.1), we thus obtain

$$f(\theta) = -\frac{2\mu}{\hbar^2 q}\int_0^\infty rV(r)\sin(qr)\,dr. \tag{4.5}$$

Eq. (4.5) is the Born approximation for short range spherical symmetric potentials.

As we have mentioned at the beginning of this section, as an example of a possible application of the method we have developed, we will set the background term, $f^{(bg)}$ in (3.22), to be equal to the the Born approximation (4.5) and study the corresponding effects.

Chapter 5

Results and Discussions

5.1 Short-range potential

The potential that will be used throughout the calculations is given by [14]

$$V(r) = 7.5r^2e^{-r}, \tag{5.1}$$

where the units of $V(r)$ and r are in MeV and fm, respectively. Observing Fig. (5.1), it can be seen that the potential dimishes exponentially and thus becomes negligible at large r.

5.2 Jost function

The Jost functions which are given by Eqs. (2.21)-(2.22) are functions of two variables i.e energy and angular momentum. However, by fixing the energy these functions depend on a single parameter which is the angular momentum. The Jost functions were calculated by, firstly, solving numerically the differential equations (2.15)-(2.16) for the unknown functions $F^{(in/out)}(E, r)$ using the Runge-Kutta-Fehlberg method (Appendix C) with the following

E(MeV)	ℓ
5.0000000000000	$1.1062512746676 + i0.3814023675897$
4.6000000000000	$0.83713208064778 + i0.22243700953498$
4.2000000000000	$0.54542142241316 + i0.10135133625993$
3.8000000000000	$0.25120839444728 + i0.032432053781362$
3.4000000000000	$-0.016997035815325 + i0.0072539908161906$
3.0000000000000	$-0.25112888414914 + i0.0012513400669567$
2.6000000000000	$-0.45931501169907 + i0.00017735937925323$

Table 5.1: The Regge trajectory obtained from the potential $V(r)$ in the complex ℓ plane by varying the energy.

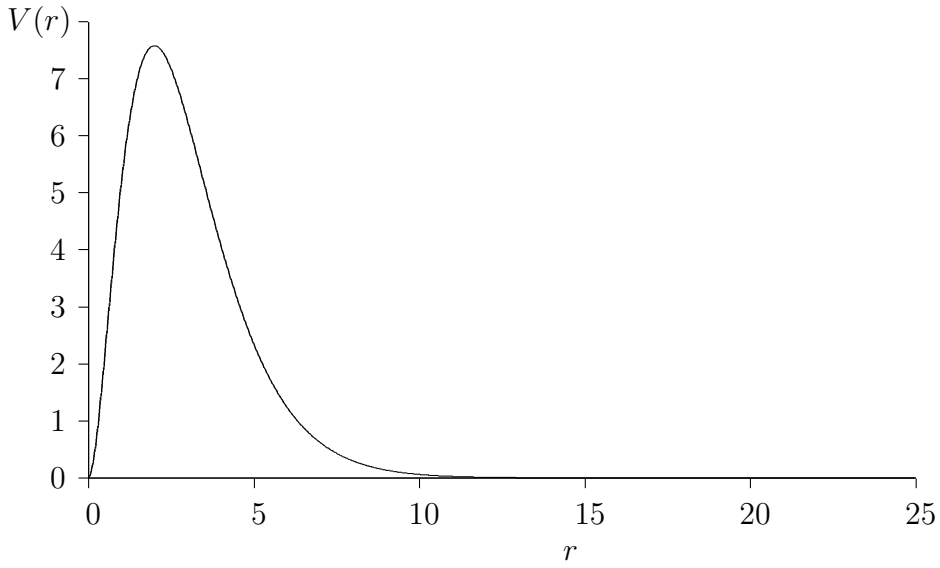

Figure 5.1: Potential (5.1) as a function of the distance between itself and the plane wave r

inputs:

- Tolerence = 10^{-13}.

$k_0(\text{fm}^{-1})$	$E_0(\text{MeV})$	$\Gamma(\text{MeV})$
$2.607681 + i2.594740 \times 10^{-9}$	3.400000	-1.353251
$3.129041 - i0.350533$	4.956885	2.193667
$3.398317 - i0.990741$	6.265062	6.733701
$3.739319 - i2.325793$	9.695911	17.393763
$3.592050 - i1.657714$	7.825422	11.909186
$3.854762 - i2.986489$	11.889156	23.024415

Table 5.2: The Zeros k_0 of the Jost functions in the complex k-plane and the corresponding energies as well as resonance width, respectively

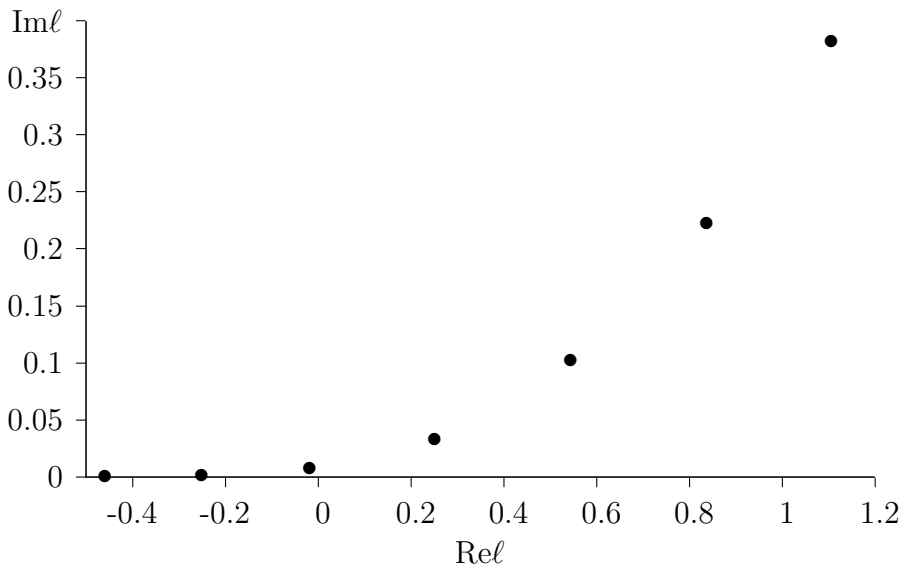

Figure 5.2: Regge trajectory for energies of 2.6MeV to 5.0 MeV in increments of 0.4 MeV

- $r_{min} = 0.1 \times 10^{-3}\,\text{fm}$ and $R = 25\,\text{fm}$.
- Intial conditions $F^{(in/out)}(E, 0) = 1$.

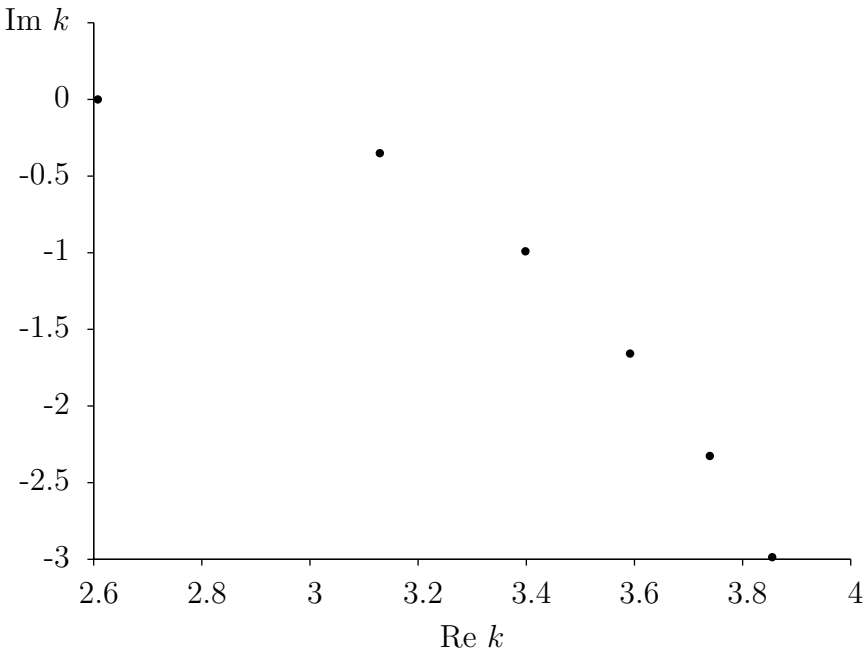

Figure 5.3: Resonance points on the complex k plane

- $h = 2.5 \times 10^{-3}$.
- energy of $E = 5$ MeV.

Finally, when $R = 25\,\text{fm}$, the unknown functions gave us the Jost functions.

The Regge trajectory is determined by tracing out the behavior of the complex momenta when the energy is increased. Fig. (5.2), shows a Regge trajectory that was calculated by starting with the energy 2.6 MeV and increasing it to 5.0 MeV in increments of 0.4 MeV. Then Newton method (Appendix D) with tolerance $= 10^{-10}$ was used to locate the corresponding ℓ values at which $f_\ell^{(in)}(E) = 0$, as shown in table (1). The values of the Regge poles that didn't satisfy the linear independence condition (2.64) were discarded.

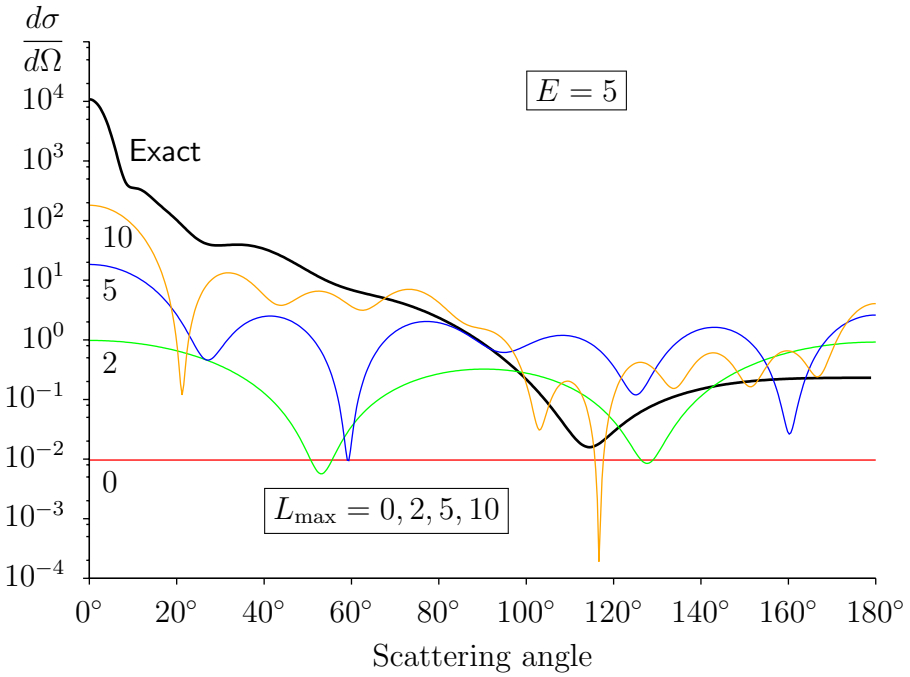

Figure 5.4: The exact differential cross section and $L = 0, 2, 5, 10$ partial waves against the scattering angle

As it can be seen from Fig. (5.2), as the energy increases the Regge poles moves to the right, thus $\ell(E)$ increases with energy. Furthermore, there are no Regge poles that are lying strictly on the $Re\,\ell$ axis - the imaginary value for the first two Regge poles are not zero, as it can been seen in table (1). As a result, there are no bound states in this trajectory. As it was mentioned on page 12, a resonance state occur when $\mathrm{Im}\,\ell$ is very small and $\mathrm{Re}\,\ell$ is equal to a non-negative integer value. From this it follows that a resonance state occurs at a point $\ell = (-0.016997035815325, 0.0072539908161906)$. This is because $\mathrm{Re}\,\ell$ is close to the non-negative integer value 0 and its imaginary part its very small.

The Jost functions are analytic with respect to the parameters ℓ and E.

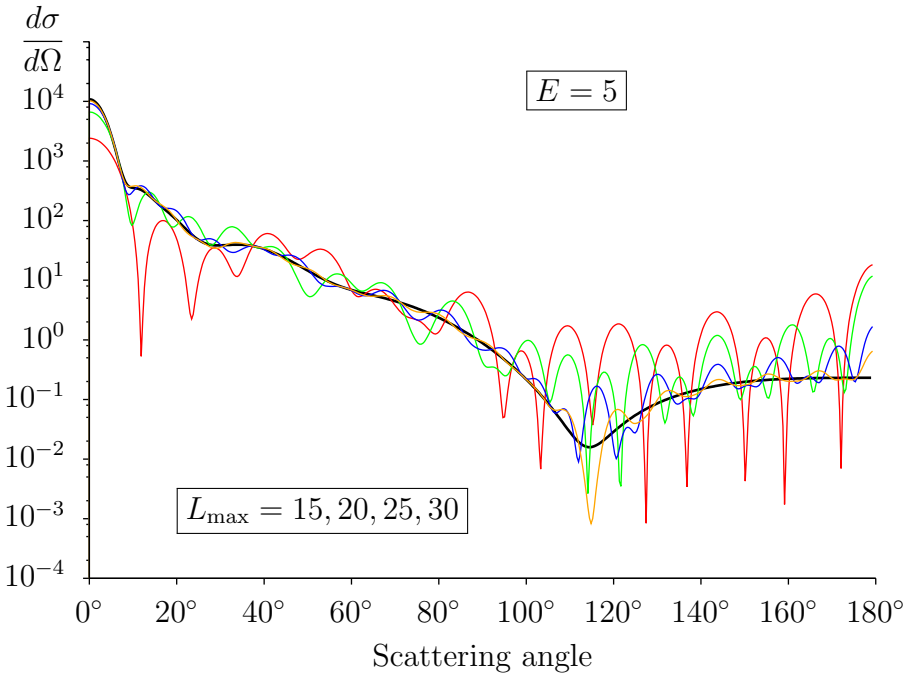

Figure 5.5: The exact differential cross section and $L = 15(\text{red}), 20(\text{green}), 25(\text{blue})$ and $30(\text{orange})$ partial waves against the scattering angle.

We have showed in the preceding paragraph that a resonance state occur when $\ell = (-0.016997035815325, 0.0072539908161906)$. By fixing ℓ at this state, the incoming Jost function, $f_\ell^{(in)}(E)$, becomes a function of a single parameter k - momentum. The resonance points on the complex k-plane that are given in table (2), were calculated by the Newton method. The equation

$$E = \frac{\hbar^2 k^2}{2m}, \tag{5.2}$$

where

$$\frac{\hbar^2}{2m} = \frac{1}{2},$$

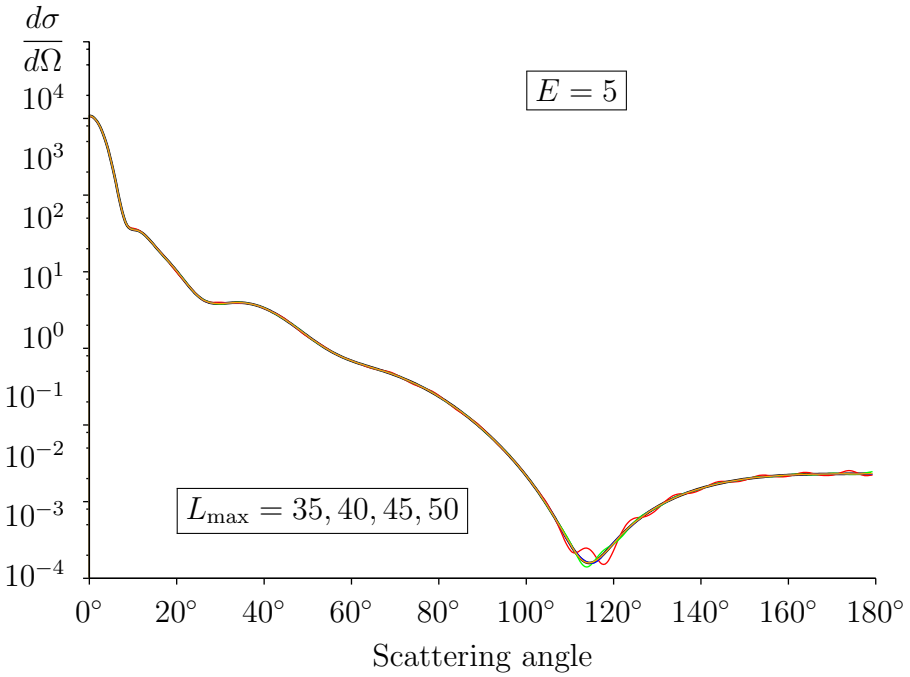

Figure 5.6: The exact differential cross section and $L = 35, 40, 45, 50$ partial waves against the scattering angle.

was used to move from momentum to energy. The resonace width Γ is given by

$$\Gamma = 2 \operatorname{Im} E.$$

And

$$E_0 = |E|.$$

The duration of a resonace state is related to Γ in the following way

$$T_{\frac{1}{2}} = \frac{\hbar \ln(2)}{\Gamma}. \tag{5.3}$$

Considering table (2), the resonance state that corresponds to $\Gamma = 2.193667$MeV will occur longer as compared to that of $\Gamma = 23.024415$MeV. This means that

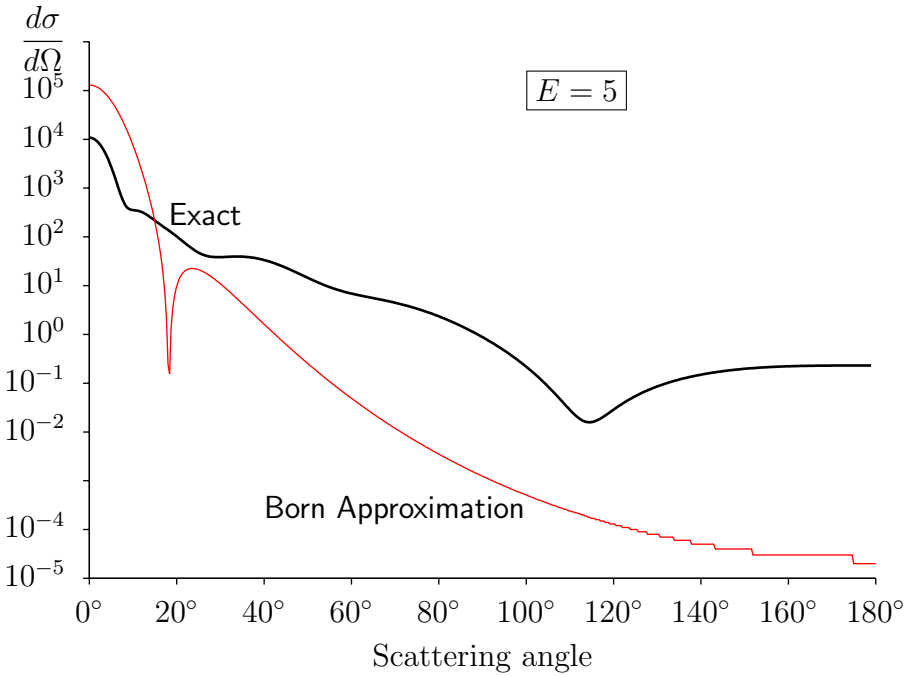

Figure 5.7: The exact differential cross section and the Born approximation against the scattering angle

small values of Γ implies that the incident plane wave will spend more time in the vicinity of the potential. On the other hand, large values of Γ implies, the plane wave will spend less time around the potential.

5.3 Partial-waves

As we have already mentioned in section 3.2 on page 32, the partial wave expansion converges slowly for scattering energies, i.e $E > 0$. We provide an illustration for the assertion that we made using the potential (5.1).

The partial waves of $\mathrm{L}_{max} = 0, 2, 5, 10$ were not enough to approximate the exact differential cross section, as it may be seen in Fig. (5.4). When

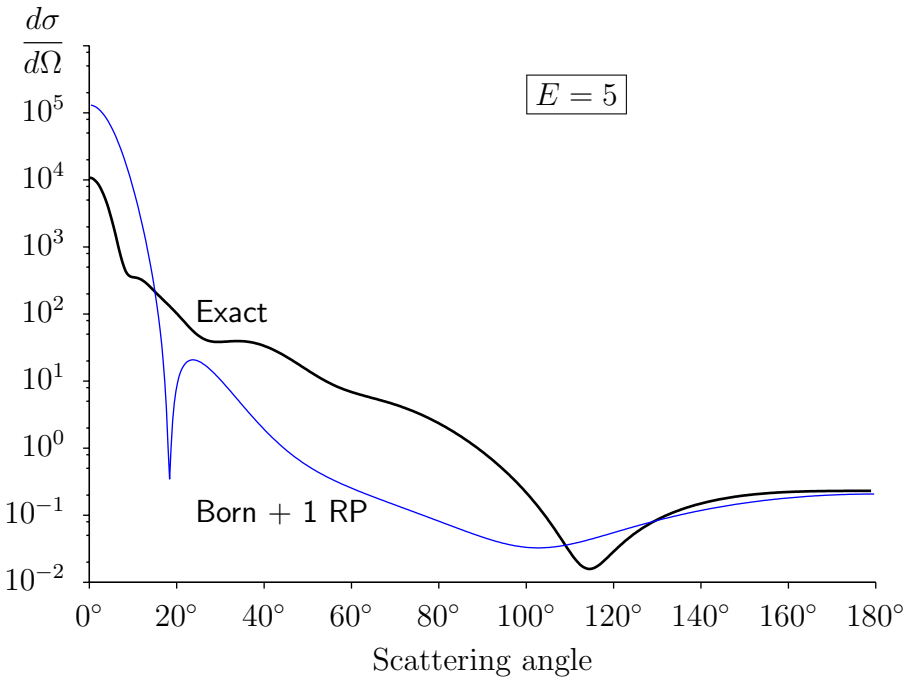

Figure 5.8: The exact differential cross section and Born approximation plus 1 Regge pole against the scattering angles

$L_{max} = 0$, the graph is horizontal, moreover, when $L_{max} = 2$ and $L_{max} = 5$ their graphs have 2 and 5 oscillations, respectively. But when $L_{max} = 10$, the number of oscillations is 9, instead of 10. Therefore, we may conclude that when $L_{max} < 10$ there is a one-to-one correspondence between L_{max} and the number of oscillations.

When $L_{max} = 15, 20, 25$ and 30, Fig. (5.5), the partial waves approaches the exact differential cross section. When $L_{max} = 50$ (51 terms), shown in Fig. (5.6), the differential cross section of the partial wave series approximates the exact differential cross section. In section 3.1 on page 28, we have

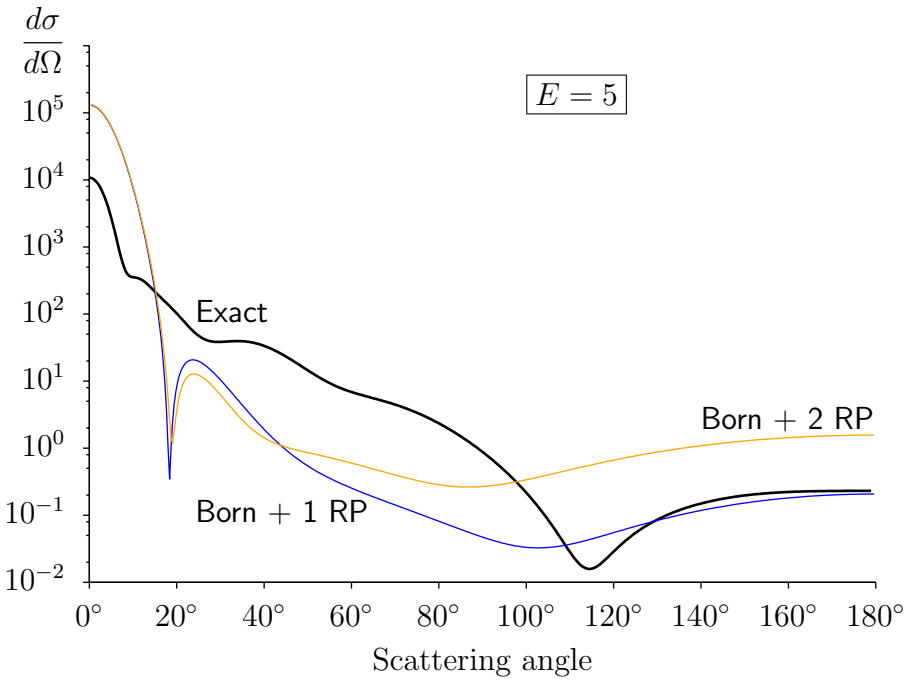

Figure 5.9: Exact differential cross section, Born approximation and 1 Regge pole (blue) and Born approximation plus 2 Regge pole (orange) against the scattering angle

established that the partial wave expansion would be useful only when

$$\mathrm{L}_{max} \leq Rk = 5 \times 25 = 125,$$

and indeed its true. This corresponds with the theory [5].

5.4 Scattering amplitude

The method we have developed allows us to express the scattering amplitude as a sum of the background and pole term (3.21). Furthermore, it proposes a way to calculate the pole term. To demostrate how this method may be

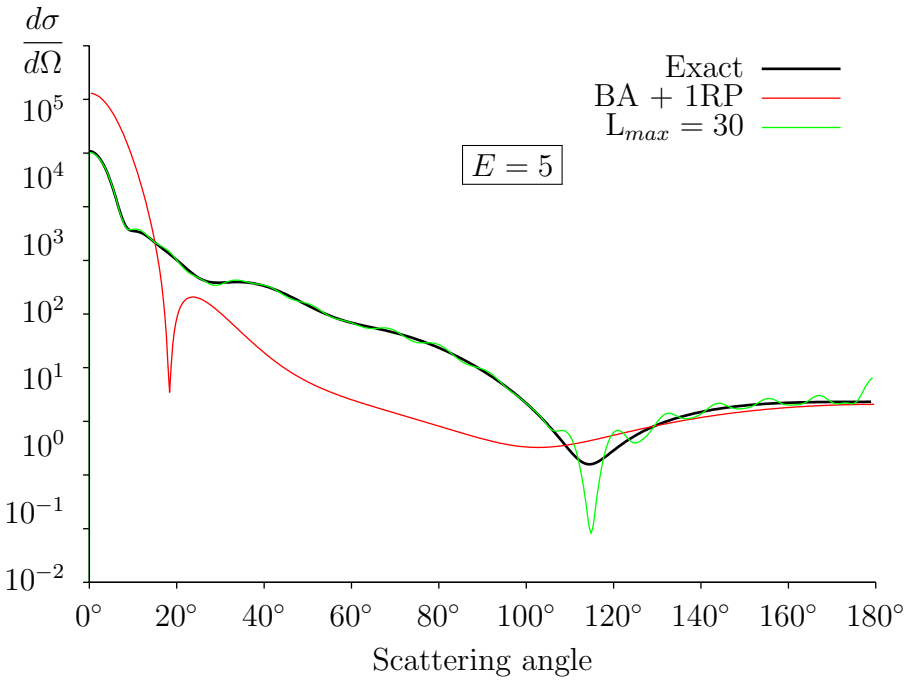

Figure 5.10: Exact differential cross section, 31 partial waves and 1 Regge pole against the scattering angle

applied, we let the background term equal the Born approximation, as suggested in Eq. (4.5) on page 43.

When the scattering amplitute was set to be the Born approximation, we obtain Fig. (5.7) and from this figure, we observe that forward scattering which occurs at $\theta = 0°$ (this does not mean that there is no scattering taking place, since the differential cross section is non-zero) its differential cross section is greater in the Born approximation as compared to the exact differential cross section, moreover, in the range $\theta \in [0°, 15°]$, the Born approximation scatters more of the incident plane wave as compared to the exact differential cross section. When $\theta \in [15°, 115°]$ both the exact differential cross section as well as the Born approximation cross section scatters less and less of the incom-

ing wave and when $\theta \in (115°, 180°]$, exact differential cross section starts to increase till it is 0.20 while Born approximation cross section continues to decay to 0.002. Thus, when the scattering amplitude is modelled by the Born approximation, it fails to approximate the exact differential cross section at large scattering angles.

When a Regge pole of $\ell = (1.1062512746676, 0.38140236758979)$ with residue $(-6.13308562672633117 \times 10^{-2}, 2.88798346067276022 \times 10^{-2})$ is added to the Born approximation, we obtain Fig. (5.8), hence by adding this pole, the tail of the Born approximation moves close to that of the exact differential cross section, thus, this Regge pole improved the Born approximation which initially failed to approximate the exact differential cross section at large scattering angles.

Adding a second Regge pole $\ell = (0.83713208064778, 0.22243700953498)$ with residue $(-9.4922270662562105 \times 10^{-2}, 5.9714033987513508 \times 10^{-2})$ to the Born approximation, results in Fig. (5.9). When $\theta > 70°$, this graph goes above that of the exact differential cross section, implying that, by adding the second Regge pole to the Born approximation, more of the incoming wave will be scattered into the solid angle $d\Omega$ as compared to exact differential cross section. The residues as well as the first Regge pole were calculated by using the energy $E = 5$ MeV, but the second Regge pole was calculated using the energy $E = 4.6$ MeV, as it is shown in table (1).

At the very beginning, the scattering amplitude was expressed as a partial wave series, with the summation variable ℓ taking only non-negative integers. When we consider 3-terms, i.e $L_{max} = 2$, we observe from Fig. (5.4) that this graph it is not a good approximation of the exact differential cross section - since the $L_{max} = 2$ curve behaves like a $|\cos\theta|$ graph. It's only

when $L_{max} = 50$ (51 terms) that the differential cross-sectional area of the partial wave series converges to that of the exact differential cross section. By allowing ℓ to take complex values, this enabled us to express the scattering amplitude as a sum of two terms, namely, the Born approximation term and the Regge pole term. Addition of a single Regge pole to the Born approximation yielded results that are nearly equivalent to adding 31 partial waves, Fig. (5.10), at large scattering angles, $\theta \geq 130°$.

As it may be seen, Fig. (5.9), when $\theta \leq 45°$ the graph of the Born approximation and a single Regge pole as well as Born approximation and two Regge poles behaves in a similar way, thus the background integral term dominates the pole term small angles. On the other hand, as more Regge poles are added to the Born approximation, the part that is most affected is when $\theta > 45°$. Therefore, the Regge pole term dominates the background term for large scattering angles, which is a result that was also obtained by [7].

We have demostrated that when our method is applied to the Born approximation, it improves it's behavior for large scattering angles. In essence, this method may be applied generally if the background term fails to approximate the cross section at large scattering angles.

Chapter 6

Conclusions

The aim of this research was to develop a method for expanding the Jost functions as a Taylor-type power series on the complex angular momentum plane. We began by defining the radial wave function in terms of unknown functions. Then transformed the Schrödinger equation of the radial wave function into a first-order coupled differential equations for the unknown functions. These functions at large distances converges to the Jost functions.

We proved that for scattering states, the Regge poles were located in the first quadrant of the complex angular momentum plane. We further proved that the Jost functions were analytic with respect to the parameter ℓ in that quadrant. These two proves enabled us to obtain a power series expansion of the Jost functions.

After expressing the Jost functions as a power series expansion the next task was to relate them to the scattering amplitude. In order to do that, we started by considering a scattering wave function that is defined at large distances, this wave function is expressed as a sum of the incident plane wave and the scattered wave. The scattering amplitude for spherical sym-

metric short range potential was written as a partial wave series where the summation variable ℓ took only non-negative integers(these integers were positioned on the $\mathrm{Re}\,\ell$-axis), moreover, the partial wave amplitude dependent on the Jost functions.

When the momentum was greater that zero, more terms of the partial wave series would be considered and as a result, the series would converge slowly. By allowing ℓ to take complex values, it was shown that for scattering processes, ℓ was located in the first quadrant of the complex angular momentum plane, then the series was converted into an integral by the Watson transformation. The properties of the S-matrix allowed us to express the scattering amplitude as a sum of two terms, namely, the background and pole term. The pole term was expressed in terms of the Regge poles and the residues. Regge poles were located by the Newton's method and residues were calculated by solving a system of first order linear differential equations for fixed values of energy and Regge pole.

To demostrate how this developed method may be used in application, we set the background term to be the Born approximation. The results of our calculations showed that the differential cross section of the partial wave series converged to that of the exact differential cross section when 51 partial waves were considered. The differential cross section of the Born approximation failed to approximate the exact differential cross section for large scattering angles. By adding a single Regge pole to the Born approximation, its differential cross section gave a better approximation of the exact differential cross section at large scattering angles - which was equivalent to adding 31 partial waves.

It was also seen that the background term dominated the pole term when

the scattering angles were less than 45°(small angles), while the pole term dominated for large scattering angles ($\theta \geq 130^{\circ}$). This conclussion was also obtained by [7]. For further studies, the developed method may be used if the differential cross section of the background term fails to converge to the exact differential cross section at large scattering angles.

Chapter 7

Appendices

7.1 Appendix A

The method of variation of parameters

The following derivation was adopted from [11] and [18].
The method of variation of parameters is useful in determining a particular solution for linear ordinary differential equations, with constant and variable coefficients. But this method requires knowledge of the complementary solution.

Suppose we want to find the solution of the nonhomogeneous differential equation

$$a(x)\frac{d^2y}{dx} + b(x)\frac{dy}{dx} + c(x)y(x) = f(x). \tag{7.1}$$

This method will be useful when $f(x), a(x), b(x)$ and $c(x)$ are continuous functions and $a(x) \neq 0$. We start by determining the complementary solution of the following homogeneous ODE

$$a(x)\frac{d^2y}{dx} + b(x)\frac{dy}{dx} + c(x)y(x) = 0, \tag{7.2}$$

which is given by

$$y_c(x) = c_1 y_1(x) + c_2 y_2(x), \tag{7.3}$$

where $y_1(x)$ and $y_2(x)$ are linearly independent solutions. Suppose that the particular solution of (7.1) is given by

$$y_p(x) = u_1(x) y_1(x) + u_2(x) y_2(x), \tag{7.4}$$

where $u_1(x)$ and $u_2(x)$ are unknown functions to be determined. $y_1(x)$ and $y_2(x)$ are the same as in Eq.(7.3).

In order to determine the unknown functions, we need to have two equations. One of which is given by Eq. (7.1) and the other is given by

$$y_1 u_1'(x) + y_2 u_2'(x) = 0, \tag{7.5}$$

where the primes indicate derivatives with respect to x and $y_i \equiv y_i(x)$. When we substitude the particular solution (7.4) into (7.1) and using the fact that

$$a y_1'' + b y_1' + c y_1 = 0 \text{ and } a y_2'' + b y_2' + c y_2 = 0,$$

we obtain

$$y_1 u_1' + y_2 u_2' = \frac{f(x)}{a(x)}.$$

Therefore, the particular solution must satisfy,

$$\begin{aligned} y_1 u_1'(x) + y_2 u_2'(x) &= 0 \\ y_1 u_1' + y_2 u_2' &= \frac{f(x)}{a(x)}. \end{aligned} \tag{7.6}$$

From (7.6), we can determine u_1' and u_2' as well as calculating the unknown functions u_1 and u_2.

7.2 Appendix B

Numerical calculation of the n^{th} derivative

Our next goal is to derive an expression of the n^{th} derivative of $h_\ell^{(\pm)}(kr)$, from (2.60), and for that we will use the Cauchy integral theorem. This theorem is stated as follows [11]; if $f(z)$ is analytic in and on the closed contour C and z_0 is a point within C, then

$$f(z_0) = \frac{1}{2\pi i} \oint_C \frac{f(z)}{z - z_0}\, dz \tag{7.7}$$

Eq. (7.7) tells us that the value of the analytic function at an arbitrary point $z_0 \in C$ is determined by the value of the function at any point in the circle. From (7.7) we have

$$f'(z_0) = \frac{1}{2\pi i} \oint_C \frac{f(z)}{(z - z_0)^2}\, dz,$$

$$f''(z_0) = \frac{2}{2\pi i} \oint_C \frac{f(z)}{(z - z_0)^3}\, dz,$$

$$f'''(z_0) = \frac{6}{2\pi i} \oint_C \frac{f(z)}{(z - z_0)^4}\, dz,$$

thus the nth derivative

$$f^{(n)}(z_0) = \frac{n!}{2\pi i} \oint_C \frac{f(z)}{(z - z_0)^{n+1}}\, dz. \tag{7.8}$$

Suppose γ is a circle centered at z_0 with radius r, as illustrated by Fig. (7.1), then any point z in γ can be expressed as

$$z = z_0 + re^{i\theta},$$

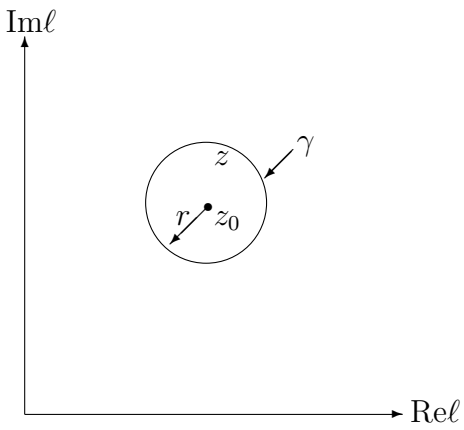

Figure 7.1: Circle γ with center z_0 with an arbitrary point z

and

$$dz = ire^{i\theta}\, d\theta.$$

Therefore (7.7)and (7.8) respectively become

$$f(z_0) = \frac{1}{2\pi}\int_0^{2\pi} f(z_0 + re^{i\theta})\, d\theta, \tag{7.9}$$

$$f^{(n)}(z_0) = \frac{n!}{2\pi}\int_0^{2\pi} \frac{f(z_0 + re^{i\theta})}{(re^{i\theta})^n}\, d\theta. \tag{7.10}$$

To approximate the integral in (7.10) we use Gauss-Legendre quadrature, which states as,

$$\int_a^b f(x)\, dx = \sum_{i=1}^{N} \omega_i f(x_i), \tag{7.11}$$

where N is the number of integration points, ω_i is the weight function defined as

$$\omega_i = \frac{2}{(1 - x_i^2)(P_n'(x_i))^2}.$$

$P_n'(x)$ is the derivative of the Legendre polynomial with respect to x and x is such that $P_n(x) = 0$. Applying (7.11) on (7.10) we obtain

$$f^{(n)}(z_0) = \frac{n!}{2\pi} \sum_{j=1}^{N} \omega_j \frac{f(z_0 + re^{i\theta(j)})}{(re^{i\theta(j)})^n}. \tag{7.12}$$

Applying (7.10) on (2.40), we obtain

$$\begin{aligned} \partial_\ell^n h_\ell^{(\pm)}(z_0) &= \partial_\ell^n j_\ell(z_0) \pm i\partial_\ell^n n_\ell(z_0) \\ &= \frac{n!}{2\pi} \int_0^{2\pi} \left(\frac{j_\ell(z_0 + re^{i\theta})}{(re^{i\theta})^n} \pm i \frac{n_\ell(z_0 + re^{i\theta})}{(re^{i\theta})^n} \right) d\theta. \end{aligned} \tag{7.13}$$

7.3 Appendix C

Runge-Kutta-Fehlberg method

For us to approximate the solution of the initial value problem

$$y' = f(t, x), \quad a \leq t \leq b, \quad y(a) = \alpha,$$

with local truncation error within a given tolerance. We use the Runge-Kutta-Fehlberg method, where numbers a and b are boundaries of the interval and α is the initial condition. This method has a local truncation error of order five [16] and its given by

$$y_{i+1} = y_i + \frac{16}{135}k_1 + \frac{6656}{12825}k_3 + \frac{28561}{56430}k_4 - \frac{9}{50}k_5 + \frac{2}{55}k_6, \tag{7.14}$$

where the variable coefficients $k_i's$ are calculated as follows ([16] and [17]):

$$\begin{aligned}
k_1 &= hf(t_i, y_i), \\
k_2 &= hf\left(t_i + \frac{h}{4}, y_i + \frac{1}{4}k_1\right), \\
k_3 &= hf\left(t_i + \frac{3h}{8}, y_i + \frac{3}{32}k_1 + \frac{9}{32}k_2\right), \\
k_4 &= hf\left(t_i + \frac{12h}{13}, y_i + \frac{1932}{2197}k_1 - \frac{7200}{2197}k_2 + \frac{7296}{2197}k_3\right), \\
k_5 &= hf\left(t_i + h, y_i + \frac{439}{216}k_1 - 8k_2 + \frac{3680}{513}k_3 - \frac{845}{4104}k_4\right), \\
k_6 &= hf\left(t_i + \frac{h}{2}, y_i - \frac{8}{27}k_1 + 2k_2 - \frac{3544}{2565}k_3 + \frac{1859}{4104}k_4 - \frac{11}{40}k_5\right).
\end{aligned}$$

Where h is the step size. According to [17], the method works in the following way:
At each step, two approximations of the solutions are computed and com-

pared. And if these approximations are in close agreement, the approximation is accepted, whereas, if the two approximations are not in agreement to a specified accurately, the stepsize will be reduced. Finally, if the approximations agree to more significant digits than required, the size will be increased. Furthermore, the optimum step size is obtained by multiplying the scalar

$$s = \left(\frac{\text{tol } h}{2|y_{i+1} - z_{i+1}|}\right)^{1/4} \approx 0.84 \left(\frac{\text{tol } h}{|y_{i+1} - z_{i+1}|}\right)^{1/4},$$

by the current step size h. Where [16]

$$z_{i+1} = y_i + \frac{25}{216}k_1 + \frac{1408}{2565}k_3 + \frac{2197}{4104}k_4 - \frac{1}{5}k_5.$$

7.4 Appendix D

Newton's method

Newton method is used to determine the zeros of a function, i.e

$$\{x : f(x) = 0\}$$

given an initial approximation x_0. The initial approximation x_0 has the following properties [16]

1. $f'(x_0) \neq 0$.
2. $|x - x_0|$ is very small.

Therefore, the Newton method is given by

$$x_{i+1} = x_i - \frac{f(x_i)}{f'(x_i)} \tag{7.15}$$

Bibliography

[1] Nouredine Zettili, Quantum Mechanics Concepts and Applications 2nd ed 2009 John Wiley & Sons, Inc.,

[2] J-L Basdevant, Jean Dalibard. Quantum Mechanics 2002 Springer Germany

[3] Eugen Merzbacher, Quantum mechanics (2nd ed.) 1970 John Wiley & Sons, Inc.,

[4] David J. Griffiths, Introduction to Quantum mechanics 2nd ed. 2005 Pearson Prentice Hall

[5] Charles J. Joachain, Quantum Collision Theory 1975 American Elsevier Publishing Company, Inc.

[6] New Theoretical Methods for Molecular Collisions : The Complex Angular-momentum Approach - Connor

[7] Title of journal: Regge description of optical model scattering Authors : T. Tamura and H.H Wolter

[8] Computational study and the complex angular momentum analysis of elastic scattering for complex optical potentials J.n.L Connor, D.C Mackay and K.E Thylwe

[9] R. A Adams, Calculus a complete course, 6th ed 2006 Pearson Addision Wesley Toronto

[10] J. R. Taylor, Scattering Theory (John Wiley Sons, Inc., New York, 1972).

[11] K.F Riley, M.P Hobson and S.J Bence, 3rd Ed.,Mathematical Methods for Physics and Engineering Cambridge university Press 2006

[12] M. Abramowitz M and A. Stegun (ed) 1964 Handbook of Mathematical Functions (Washington, DC: NBS)

[13] Y.A Brychkov 2008, Handbook of Special functions, CRC Press

[14] S. A. Sofianos and S. A. Rakityansky,"Exact method for locating potential resonances and Regge trajectories", J. Phys. A30 (1977) 3725

[15] Sitenko A G 1991 Scattering Theory (Heidelberg: Springer)

[16] R.L Burden, J.D Faires, Numerical Analysis 9th ed. 2011

[17] J.H Mathews and K.K Fink, Numerical analysis using Matlab, 4th ed. 2004 Prentice-Hall inc. New Jersey

[18] http://howellkb.uah.edu/DEtext/Part3/Var$_P arameter.pdf$